Stable carbon isotope gradients in benthic foraminifera as proxy for organic carbon fluxes in the Mediterranean Sea

Marc Theodor[a,*], Gerhard Schmiedl[a], Frans Jorissen[b], and Andreas Mackensen[c]

[a] Center for Earth System Research and Sustainability, Institute of Geology, University of Hamburg, Bundesstrasse 55, D-20146 Hamburg, Germany

[b] CNRS, UMR 6112, LPG–BIAF, Recent and Fossil Bio-Indicators, Université d'Angers, 2 Boulevard Lavoisier, 49045 Angers Cedex, France

[c] Alfred Wegener Institute Helmholtz Centre for Polar and Marine Research, Am Alten Hafen 26, D-27568 Bremerhaven, Germany

[*] Corresponding author

E-mail addresses: marc.theodor@uni-hamburg.de (M. Theodor), gerhard.schmiedl@uni-hamburg.de (G. Schmiedl), frans.jorissen@univ-angers.fr (F. Jorissen), andreas.mackensen@awi.de (A. Mackensen)

Abstract

We have determined stable carbon isotope ratios of epifaunal and shallow infaunal benthic foraminifera in the Mediterranean Sea to relate the inferred gradient of pore water $\delta^{13}C_{DIC}$ to varying trophic conditions. This is a prerequisite for developing this difference into a potential transfer function for organic matter flux rates. The data set is based on samples retrieved from a well-defined bathymetric range (400–1500m water depth) of sub-basins in the western, central and eastern Mediterranean Sea. Regional contrasts in organic matter fluxes and associated $\delta^{13}C_{DIC}$ of pore water are recorded by the $\delta^{13}C$ difference ($\Delta\delta^{13}C_{Umed\text{-}Epi}$) between the shallow infaunal *Uvigerina mediterranea* and epifaunal species (*Planulina ariminensis*, *Cibicidoides pachydermus, Cibicides lobatulus)*. Within epifaunal taxa, highest $\delta^{13}C$ values are recorded for *P. ariminensis,* providing the best indicator for bottom water $\delta^{13}C_{DIC}$. In contrast, *C. pachydermus* reveals minor pore water effects at the more eutrophic sites. Because of ontogenetic trends in the $\delta^{13}C$ signal of *U. mediterranea* of up to 1.04‰, only tests larger than 600µm were used for the development of the transfer function. The recorded differences in the $\delta^{13}C$ values of *U. mediterranea* and epifaunal taxa ($\Delta\delta^{13}C_{Umed\text{-}Epi}$) range from -0.46 to -2.13‰, with generally higher offsets at more eutrophic sites. The measured $\delta^{13}C$ differences are related to site-specific differences in microhabitat, depth of the principal sedimentary redox boundary, and TOC content of the ambient sediment. The $\Delta\delta^{13}C_{Umed\text{-}Epi}$ values reveal a consistent relation to C_{org} fluxes estimated from satellite-derived surface water primary production in open-marine settings of the Alboran Sea, Mallorca Channel, Strait of Sicily and southern Aegean Sea. In contrast, $\Delta\delta^{13}C_{Umed\text{-}Epi}$ values in areas affected by intense resuspension and riverine organic matter sources of the northern to central Aegean Sea and the canyon systems of the Gulf of Lions suggest higher C_{org} fluxes compared to the values based on recent primary production. Taking regional biases and uncertainties into account, we establish a first $\Delta\delta^{13}C_{Umed\text{-}Epi}$ based transfer function for C_{org} fluxes for the Mediterranean Sea.

Key words: benthic foraminifera, stable carbon isotopes, microhabitat, organic matter fluxes, Mediterranean Sea, transfer function

1. Introduction

The stable isotope composition of benthic foraminifera is used in a wide range of paleoceanographic applications. The $\delta^{18}O$ signal of benthic foraminifera provides information on bottom water temperature and salinity, and has been applied to estimate global ice volume changes (e.g. Shackleton & Opdyke, 1973; Adkins et al., 2002; Marchitto et al., 2014). The benthic foraminiferal $\delta^{13}C$ signal is mainly used for the reconstruction of changes in deep-sea circulation, bottom water oxygen concentrations, and organic carbon fluxes to the sea floor (Curry & Lohmann, 1982; Zahn et al., 1986; McCorkle & Emerson, 1988; Mackensen & Bickert, 1999; Pahnke & Zahn, 2005). Recently, more quantitative approaches have been applied to the reconstruction of past changes in deep-water oxygenation (Stott et al., 2000; Schmiedl & Mackensen, 2006; Hoogakker et al., 2015). There have also been attempts to use multi-species $\delta^{13}C$ records to reconstruct past organic carbon fluxes (Zahn et al., 1986; Schilman et al., 2003; Kuhnt et al., 2008). However, all of these studies lack a regional calibration based on living specimens and modern organic carbon flux data.

The $\delta^{13}C$ gradient of pore water dissolved inorganic carbon (DIC) in the uppermost surface sediment is directly related to the flux and decomposition rates of organic matter (McCorkle & Emerson, 1988; McCorkle et al., 1990; Holsten et al., 2004). With increasing depth in the sediment more ^{13}C depleted organic matter ($\delta^{13}C$ around -18 to -23‰, e.g. Mackensen, 2008) is remineralized by microbial activity (McCorkle et al., 1985). This process results in $\delta^{13}C_{DIC}$ pore water depletions of up to -4‰ relative to the bottom water signal (McCorkle & Emerson, 1988; McCorkle et al., 1990; Holsten et al., 2004). The preferential release of ^{12}C to the pore water stops when no more OM is remineralized, which mostly coincides with the total consumption of electron acceptors, of which oxygen, nitrate and sulfate are the most energy-efficient ones (McCorkle & Emerson, 1988; McCorkle et al., 1990; Koho & Pina–Ochoa, 2012, Hoogakker et al., 2015).

The $\delta^{13}C_{DIC}$ pore water gradient is reflected in the $\delta^{13}C$ signal of benthic foraminifera from defined microhabitats on and below the sediment–water interface (Grossman, 1984a; b; McCorkle et al., 1990; 1997; Rathburn et al., 1996; Mackensen & Licari, 2004; Schmiedl et al.,

2004; Fontanier et al., 2006). Although benthic foraminifera can migrate through the sediment (Linke & Lutze, 1993; Ohga & Kitazato, 1997) and living individuals may occur across a relatively wide depth interval, the $\delta^{13}C$ of a species exhibits relatively little scatter, and all specimens tend to reflect the same calcification depth (Mackensen & Douglas, 1989; McCorkle et al., 1990, 1997; Mackensen et al., 2000; Schmiedl et al., 2004). The study of McCorkle & Emerson (1988) has shown that the difference between $\delta^{13}C_{DIC}$ of bottom water and $\delta^{13}C_{DIC}$ of pore water at the depth in the sediment where oxygen approaches zero is directly related to the oxygen content of the bottom water mass. Based on this observation, the $\delta^{13}C$ difference of epifaunal (e.g. *Cibicidoides*) and deep infaunal (*Globobulimina*) taxa was used as proxy for the quantification of past changes in deep-water oxygenation (Schmiedl & Mackensen, 2006; Hoogakker et al., 2015). In well-oxygenated bottom waters, enhanced organic matter fluxes and decomposition rates result in steepening $\delta^{13}C_{DIC}$ gradients in the uppermost sediment, which is then reflected by the $\delta^{13}C$ difference between epifaunal and shallow infaunal (e.g., *Uvigerina*) species (Zahn et al. 1986; Mackensen et al., 2000; Brückner & Mackensen, 2008). A simple relation between observed $\delta^{13}C$ gradients and organic matter fluxes is obscured by the ability of infaunal species to shift their microhabitat in response to changing trophic conditions (Schmiedl & Mackensen, 2006; Theodor et al., 2016). Interspecific differences in the $\delta^{13}C$ composition of benthic foraminifera are further influenced by species-specific "vital effects", which can be as large as 1‰ (Schmiedl et al., 2004; McCorkle et al., 2008; Brückner & Mackensen, 2008) and are a reflection of metabolic processes and test calcification rates (McConnaughey, 1989a; b). Of minor impact, but still traceable, is the influence of carbonate ion concentration and alkalinity gradients in pore waters (Bemis et al., 1998). Finally, significant ontogenetic $\delta^{13}C$ trends have been documented for certain taxa, particularly for the genera *Uvigerina* and *Bolivina* (Schmiedl et al. 2004; Schumacher et al., 2010; Theodor et al., 2016).

The complexity of factors influencing the stable isotope composition of deep-sea benthic foraminifera and differences between species in different depths in the sediment motivates isotopic studies on living foraminifera in relation to their biology and microhabitat. In particular, combined ecological and biogeochemical studies on a statistically relevant number of sites and

on live specimens from areas with well-defined environmental gradients are required for the establishment of reference data sets and transfer functions that could then be used for a more quantitative assessment of organic matter fluxes. The Mediterranean Sea is particularly suitable for such a study because the present deep-sea environments are characterized by systematically high oxygen contents along a gradient of trophic differences. In all basins, sub-surface water masses are highly oxygenated with O_2 concentrations of >160µmolkg^{-1} due to frequent replenishment of intermediate water in the Levantine Sea and deep water in the Gulf of Lions, Adriatic Sea, and Aegean Sea (Wüst, 1961; Lascaratos et al., 1999; Pinardi & Masetti, 2000; Tanhua et al., 2013; Pinardi et al., 2015). The inflow of nutrients with Atlantic surface waters causes an overall west-east gradient in primary production, from values of about 225gCm^{-2}yr^{-1} in the Alboran Sea to about 40gCm^{-2}yr^{-1} in the extremely nutrient-depleted oligotrophic Levantine Basin (Bosc et al., 2004; Lopez–Sandoval et al., 2011; Puyo–Pay et al., 2011; Huertas et al., 2012; Tanhua et al., 2013, Gogou et al., 2014). In areas influenced by nutrient input of larger rivers and Black Sea outflow, primary production can be locally enhanced, for example leading to a trend of decreasing primary production values along a N-S transect in the Aegean Sea (Lykousis et al., 2002; Skliris et al., 2010). In addition, resuspension and lateral transport of organic matter can lead to locally enhanced food availability in submarine canyons and isolated basins (Puig & Palanques, 1998; Danovaro et al., 1999; Heussner et al., 2006; Canals et al., 2013).

In this study we have compiled a data set on the stable carbon isotope composition of living and dead individuals of three epifaunal species (*Cibicidoides pachydermus*, *Planulina ariminensis*, *Cibicides lobatulus*) and one shallow infaunal species (*Uvigerina mediterranea*) from 19 Mediterranean sites. The sites are located in a well-defined depth interval (between 400 and 1500m) and represent a wide range of trophic conditions. Adjusted for ontogenetic effects, the $\Delta\delta^{13}C_{Umed\text{-}Epi}$ signal was compared to the microhabitat of *U. mediterranea*, the depth of the main redox boundary, TOC content, and organic carbon flux rates calculated from satellite-derived primary production or (if available) flux measurements from sediment trap studies. Major objective of this study is the development and evaluation of a transfer function

for organic matter fluxes applicable to the quantification of past trophic changes in the Mediterranean Sea.

2. Material and methods

This study is based on a compilation of new and published isotope data of multicorer samples retrieved from various Mediterranean sub-basins covering a water depth range of 424 to 1466m (Table 1). The study areas include the Alboran Sea and the Mallorca Channel (R.V. *Meteor* cruise M69/1 in August 2006, Hübscher et al., 2010; data published in Theodor et al., 2016), the Gulf of Lions, Spanish Slope off Barcelona and Strait of Sicily (M40/4 in February 1998, Hieke et al., 1999; this study and data published in Schmiedl et al., 2004), and the Aegean Sea (M51/3 in November 2001, Hemleben et al., 2003; this study) (Fig. 1). For each station, the sediment color change from yellowish brown to greenish gray was used as an indicator for the change in redox potential from positive to negative values, which serves as an approximation of oxygen consumption and penetration in the surface sediment (Lyle, 1983; Schmiedl et al., 2000).

The upper 10cm of the sediment were commonly sliced into 0.5 to 1cm intervals, in the Aegean Sea into coarser intervals below 3cm, and all samples were subsequently preserved in Rose Bengal stained alcohol (1.5g Rose Bengal per 1l of 96% ethanol) in order to stain cytoplasm of living or recently living foraminifera (Walton, 1952; Bernhard, 2000). In the laboratory, the sediment samples were wet-sieved over a 63µm sieve and, after drying at 40°C, dry-sieved over a 150µm (Aegean Sea samples) or 125µm (remaining samples) mesh, respectively. From the coarse fraction of the different down-core intervals, stained individuals of selected epifaunal and shallow infaunal taxa were counted and the Median Living Depths (MLD; Theodor et al. 2016) were calculated as reference for the respective microhabitat preferences. Only tests with at least three subsequent brightly red colored chambers were considered as living. The low number of stained individuals of epifaunal taxa impeded

157 analyses, except for Site 540B, where stained tests of *C. pachydermus* were available.
158 Likewise, stained tests of *U. mediterranea* were absent at Sites 586 and 589.

159 For stable isotope measurements, stained tests (and unstained tests if no stained tests
160 were available) of three epifaunal species (*C. pachydermus*, *P. ariminensis*, *C. lobatulus*) and
161 one shallow infaunal species (*U. mediterranea*) were selected and each test was measured
162 using an optical micrometer with an accuracy of 10µm. In total, 2 stained and 63 unstained
163 epifaunal tests as well as 155 stained and 197 unstained tests of *U. mediterranea* were
164 measured. Individual numbers of tests measured were 1-6 for *C. pachydermus*, 1-5 for *P.*
165 *ariminensis*, 1-5 for *C. lobatulus*, and 1-8 for *U. mediterranea*. The stable carbon and oxygen
166 isotope measurements were performed at the Alfred Wegener Institute, Helmholtz Centre for
167 Polar and Marine Research at Bremerhaven with two Finnigan MAT 253 stable isotope ratio
168 mass spectrometers coupled to automatic carbonate preparation devices (Kiel IV). The mass
169 spectrometers were calibrated via international standard NBS 19 to the PDB scale, with results
170 given in δ-notation versus VPDB. Based on an internal laboratory standard (Solnhofen
171 limestone) measured over a one-year period together with samples, the precision of stable
172 isotope measurements was better than 0.06‰ and 0.08‰ for carbon and oxygen, respectively.
173 The $\delta^{13}C$ difference between epi- and shallow infaunal taxa was calculated as a proxy for the
174 difference in $\delta^{13}C$ in DIC of bottom and shallow pore water. For *U. mediterranea* this procedure
175 was restricted to measurements from the size fraction >600µm in order to minimize ontogenetic
176 effects (Schmiedl et al., 2004; Theodor et al., 2016).

177 Total organic carbon (TOC) concentration in the surface sediment was measured with
178 a Carlo Erba 1500 CNS Analyzer with a precision of 0.02% on weighted sample splits in tin
179 capsules. Before measurement, $CaCO_3$ was removed from these weighted samples by adding
180 1N HCl. The TOC values of Sites 596, 601 and 602 were taken from Möbius et al. (2010a, b).
181 Bottom water oxygen concentrations are based on CTD measurements stored in the MedAtlas
182 data set. Primary productivity values in surface waters of the year preceding the sampling at
183 each site are based on satellite data of the GlobColour project, and were calculated with the
184 algorithms of Antoine & Morel (1996) as well as Uitz et al. (2008). If available, these estimates

were compared with nearby direct primary productivity and export flux measurements. The export fluxes down to the sea floor were estimated according to the function of Betzer et al. (1984) adapted by Felix (2014).

3. Results

Benthic foraminiferal $\delta^{13}C$ values of our samples cover a range of more than 3‰, with higher average values of epifaunal species than shallow infaunal *Uvigerina mediterranea* (Table 2). The epifaunal species *Cibicidoides pachydermus, Cibicides lobatulus* and *Planulina ariminensis* show average values between 1.90‰ at Site 586 (southern Aegean Sea) and -0.16‰ at Site 347 (Mallorca Channel) (Table 2; Fig. 2). The highest average epifaunal $\delta^{13}C_{Epi}$ values are in the southern and central Aegean Sea (Sites 586, 595), while further to the north at Site 602 (northern Aegean Sea) the average $\delta^{13}C_{Epi}$ value of 0.87‰ is among the lowest measured. At Site 540B in the Gulf of Lions, the average $\delta^{13}C_{Epi}$ value of 1.01‰ is in good agreement with 1.00‰ measured by Schmiedl et al. (2004) at the same site. Size-dependent measurements did not reveal any ontogenetic trend in the $\delta^{13}C$ signal of the epifaunal taxa (supplementary. table 1).

For *U. mediterranea* $\delta^{13}C_{Umed}$ values vary between -1.41 and 0.85‰ for stained tests and between -1.52 and 1.77‰ for unstained tests (Supplementary Table 1). The highest average values are recorded in the southern Aegean Sea, with 0.58‰ and 1.11‰ for stained and unstained tests, respectively. The lowest average values are recorded for the northern Aegean Sea, with -0.98‰ and -1.13‰ for stained and unstained tests, respectively. The variability at a single site reaches 1.38‰ in stained (Site 537) and 2.21‰ in unstained tests (Site 586). The ontogenetic $\delta^{13}C_{Umed}$ trends are generally comparable in the western Mediterranean Sea and the Strait of Sicily, with 0.11 ± 0.03‰ $100\mu m^{-1}$ for stained and 0.07 ± 0.03‰ $100\mu m^{-1}$ for unstained tests, except for Site 396 that shows an anomalous negative trend (Table 3; Fig. 3). In the Aegean Sea, the ontogenetic $\delta^{13}C_{Umed}$ trends are approximately 50 % steeper with an increase of 0.16 ± 0.04‰ $100\mu m^{-1}$ for stained tests. Unstained tests

212 reveal a higher variability and a less steep slope of 0.10 ± 0.07‰ 100µm^{-1} (Table 3, Fig. 3). In
213 order to avoid bias due to ontogenetic effects, only $\delta^{13}C$ values of *U. mediterranea* tests larger
214 than 600µm were used for comparison with $\delta^{13}C_{Epi}$ values.

215 The calculated $\Delta\delta^{13}C_{Umed\text{-}Epi}$ values for stained tests range from -0.64‰ in the Gulf of
216 Lion (slope Site) and -0.74‰ (Site 585) to -1.29‰ in the western Mediterranean Sea (sites 347
217 & 540A), to -1.85‰ in the northern Aegean Sea (Site 602) (Table 2). Due to the wider scattering
218 of the $\delta^{13}C$ values of unstained tests, $\Delta\delta^{13}C_{Umed\text{-}Epi}$ values range from -0.61‰ (Site 589) to -
219 2.0‰ (Site 602) in the Aegean Sea and from -0.55‰ (Site 540B) to -1.06‰ (Site 339) in the
220 western Mediterranean Sea and the Strait of Sicily (Table 2). The magnitude of $\Delta\delta^{13}C_{Umed\text{-}Epi}$
221 values exhibits a relation with trophic conditions at each site, revealing higher values at more
222 eutrophic sites.

223 The Median Living Depth of the shallow infaunal U. mediterranea (MLD_{Umed}) is used
224 here to describe its microhabitat and generally increases at sites with deep main redox
225 boundaries, at least in the western Mediterranean Sea. The deepest MLD_{Umed} are 2.13 and
226 2.25cm in the southern Aegean Sea, while the shallowest depths of 0.27cm and 0.38cm are
227 recorded in the central and northern Aegean Sea, respectively (Table 1). In the Gulf of Lions,
228 the MLD_{Umed} is between 0.43 and 0.49cm in the axis of the Lacaze–Duthiers Canyon and
229 around 1.22cm on the open slope (Table 1, Fig. 4a). The depth of the sediment color change,
230 which marks the shift in redox potential and thus oxygen penetration, ranges from 2.25cm in
231 the Gulf of Lions (Site 540A) to as much as 30cm in the central Aegean Sea (Site 596) (Table
232 1, Fig. 4b). The measured TOC contents of the surface sediment range from 0.41% (Site 586,
233 southern Aegean Sea) and 0.58% (Site 537, Strait of Sicily) to a maximum of 0.82% (Site 602,
234 northern Aegean Sea) (Table 1, Fig. 4c). The $\Delta\delta^{13}C_{Umed\text{-}Epi}$ and the MLD_{Umed} (Fig. 4a) as well
235 as the main redox boundary depth (Fig. 4b) show good correspondence, whereas the link to
236 %TOC is less distinct (Fig. 4c).

237 The estimated values for annual Primary Production (PP) range from 106 to
238 294gCm^{-2}a^{-1}. Application of the different algorithms of Antoine & Morel (1996) and Uitz et al.
239 (2008) resulted in an average offset of 54gCm^{-2}a^{-1}, with PP values consistently higher when

applying the algorithm of Antoine & Morel (1996). The highest PP values occur in the Alboran Sea (274–294 versus 192–207gCm^{-2}a^{-1} according to Uitz et al., 2008) and the northern Aegean Sea (196–237 resp. 139–164gCm^{-2}a^{-1}), while the lowest PP values occur in the southern and central Aegean Sea (151–161 resp. 106–116gCm^{-2}a^{-1}) (Table 1).

4. Discussion

4.1. Stable carbon isotope signal of epifaunal foraminifera in relation to surrounding water masses

The $\delta^{13}C$ of *Cibicidoides pachydermus*, *Cibicides lobatulus,* and *Planulina ariminensis* seems to reflect the $\delta^{13}C_{DIC}$ of the ambient bottom water since these species prefer an epifaunal microhabitat (Lutze & Thiel, 1989; Kitazato, 1994; Schmiedl et al., 2000). Comparison with published water $\delta^{13}C_{DIC}$ measurements confirms that $\delta^{13}C_{Epi}$ values are a possible bottom water proxy for the Mediterranean Sea (Pierre, 1999; Schmiedl et al., 2004; Theodor et al., 2016). Further, our new data corroborate previous observations that ontogenetic effects in the $\delta^{13}C_{Epi}$ signal of these taxa are lacking (Corliss et al., 2002; Franco–Fraguas et al., 2011; Theodor et al., 2016) (Supplementary Table 1).

Because of the lack of stained epifaunal tests at most sites, unstained tests were integrated into the analysis. For empty tests a shift to higher $\delta^{13}C_{Epi}$ values due to potential dissolution effects should be considered (Edgar et al., 2013). In addition, reworked or allochtonous tests can bias the results as documented for the $\delta^{13}C_{Cpachy}$ of Site 396 in the Mallorca Channel. At this site, fossil tests have been admixed in the surface sediment as indicated by heavy $\delta^{18}O$ values of >4.0‰ (Supplementary Table 1). In the Alboran Sea (Sites 339 and 347), we measured inter-specific epifaunal $\delta^{13}C$ differences of up to 1.4‰. This variability is a result of implausibly low $\delta^{13}C_{Clob}$ values, probably due to a relocation from shallower depths closer to the coast. These unrealistic $\delta^{13}C_{Cpachy}$ and $\delta^{13}C_{Clob}$ values were omitted for $\delta^{13}C_{Epi}$ estimation. In order to minimize these biases, a large number of tests were measured, which was possible for *C. pachydermus* and *P. ariminensis,* showing commonly

0.3–0.5‰ higher $\delta^{13}C$ values for the latter species (Table 2, Fig. 2a). Despite the aforementioned uncertainties, data of *C. lobatulus* were used to estimate $\delta^{13}C_{Epi}$ at the Mallorca Channel Sites 394 and 395, when no tests of other species were available for analysis (Theodor et al., 2016). For proper $\delta^{13}C_{Epi}$ estimation of Sites 394 and 395 the difference between $\delta^{13}C_{Pari}$ and $\delta^{13}C_{Clob}$ ($\Delta\delta^{13}C_{Pari\text{-}Clob}$ = 0.30‰) at sSite 396 was added to the $\delta^{13}C_{Clob}$ values (Table 2; Fig. 2a).

The $\delta^{13}C$ offset between *C. pachydermus* and *P. ariminensis* is not constant and appears to increase at sites with deep main redox boundaries. This suggests a connection with increasing organic matter availability and the varying offsets can be attributed to slight differences in their microhabitat (Table 2; Fig. 2a). While *P. ariminensis* is a strictly epifaunal species, living attached on surfaces or above the sediment (Lutze & Thiel, 1989), *C. pachydermus* commonly lives at or slightly below the sediment–water interface (Rathburn & Corliss, 1994; Schmiedl et al. 2000; Licari & Mackensen, 2005). A very shallow infaunal microhabitat of *C. pachydermus* is corroborated by slightly lower $\delta^{13}C$ values relative to bottom water $\delta^{13}C_{DIC}$ suggesting pore water influence (Schmiedl et al., 2004; Fontanier et al., 2006). In order to compensate for potential pore water effects in the $\delta^{13}C$ signal of the epifaunal species, the highest $\delta^{13}C_{Epi}$ values, mostly of *P. ariminensis*, should be selected for further comparison with shallow infaunal $\delta^{13}C_{Umed}$ signals. This strategy could not always be realized, either due to the lack of *P. ariminensis* (Sites 537, 601, Canyon, and Slope) or when lower $\delta^{13}C$ values were recorded for *P. ariminensis* relative to *C. pachydermus* (Site 540C). In these cases, bottom water $\delta^{13}C_{DIC}$ measurements (Canyon, Slope; from Schmiedl et al., 2004), the addition of the $\Delta\delta^{13}C_{Pari\text{-}Cpachy}$ value of the nearby Site 602 (for correction of Site 601) or the $\delta^{13}C_{Cpachy}$ values (Sites 537, 540C) were used, accepting possible deviations of $\delta^{13}C_{Epi}$ from bottom water $\delta^{13}C_{DIC}$ (Table 2).

The applied $\delta^{13}C_{Epi}$ values are related to different Mediterranean water masses (Fig. 2b). The $\delta^{13}C_{Epi}$ values of the Gulf of Lions and the Spanish continental slope off Barcelona are around 1.0‰ matching the $\delta^{13}C_{DIC}$ signature of upper Western Mediterranean Deep Water (WMDW) (Pierre, 1999). Likewise, the slightly higher $\delta^{13}C_{Epi}$ values of 1.1‰ in the Strait of

295 Sicily fall in the range of $\delta^{13}C_{DIC}$ values of intermediate waters from the Eastern Mediterranean
296 Sea and reflect the transitional setting of this area. In contrast, the $\delta^{13}C_{Epi}$ values of the Mallorca
297 Channel and the Alboran Sea are even higher than those recorded for the Eastern
298 Mediterranean Sea (Fig. 2b). This inconsistent isotope pattern likely reflects a shift in deep-
299 water formation in the Eastern Mediterranean during the 1990s, the so called Eastern
300 Mediterranean Transient (EMT; Roether et al., 2007). The EMT was accompanied by an
301 enhanced deep-water formation in the Aegean Sea and also fostered a complete renewal of
302 Western Mediterranean Sea Deep Water (WMDW) during the mid-2000s (Schroeder et al.,
303 2006; 2008). Unfortunately, the imprint of WMDW change on $\delta^{13}C_{DIC}$ of the water mass was
304 not documented, but it should have affected the sites sampled after this transition, i.e. during
305 Meteor cruise M69/1 in 2006.
306 The broad range of recorded $\delta^{13}C_{Epi}$ values of 0.87 to 1.95‰ in the Aegean Sea reflects
307 the strong small-scale oceanographic differences of this region, including presence of various
308 small isolated basins (Figs. 1, 2b). The comparatively high $\delta^{13}C_{Epi}$ values of the shallower sites
309 indicate intensified vertical convection at sites of subsurface-water formation, which recently
310 resumed after the stagnation phase of 1994 to 2000 (Androulidakis et al., 2012), although the
311 main deep-water formation area is restricted to the Cretan Sea (Roether et al., 1996;
312 Lascaratos et al., 1999). Reduced replenishment of bottom waters at greater depth of isolated
313 basins (Zervakis et al., 2003; Velaoras & Lascaratos, 2005) is accompanied by relatively low
314 $\delta^{13}C_{DIC}$ and accordingly low $\delta^{13}C_{Epi}$ values in these environments.
315
316 **4.2. Biological and environmental effects on the stable carbon isotope signal of**
317 ***Uvigerina mediterranea***
318 Size-dependent changes in the $\delta^{13}C$ signal of *Uvigerina mediterranea* are attributed to
319 ontogenetic effects. Small tests are depleted in ^{13}C, while larger tests are closer to $\delta^{13}C_{DIC}$ of
320 the ambient pore water (Fig. 3). Relatively low $\delta^{13}C_{Umed}$ values of small tests suggest stronger
321 metabolic fractionation in younger individuals (Schmiedl et al., 2004; McCorkle et al., 2008;
322 Schumacher et al., 2010; Theodor et al., 2016). A linear ontogenetic increase of 0.11‰100µm^{-}

$^{-1}$ was observed at all sites of the western Mediterranean Sea, while a steeper slope of 0.16‰100µm^{-1} was recorded in the Aegean Sea (Fig. 3). In addition, the $\delta^{13}C_{Umed}$ values of small individuals from the Aegean Sea were of order 1‰ lower compared to those from the western Mediterranean Sea.

Differences in ontogenetic $\delta^{13}C$ slopes of the related species *U. peregrina* have been attributed to its highly opportunistic response to regional contrasts in organic matter quantity and quality, and seasonality of supply (Theodor et al., 2016). Obviously, similar effects are also operational in ontogenetic $\delta^{13}C$ trends of *U. mediterranea*. In the Aegean Sea, this species appears to respond to strong seasonal contrasts in organic matter fluxes (Siokou–Frangou et al., 2002) resulting in particularly high metabolic activity and low $\delta^{13}C_{Umed}$ values in young individuals. A steepening of the $\delta^{13}C_{Umed}$ slopes from the North to the South Aegean Sea has probably the same reasons as for *U. peregrina* in the Western Mediterranean Sea. Because of the higher number of measured tests, this shift of the slope angles is more obvious in unstained than stained tests (Fig. 3). Although the number of sites was larger than in Theodor et al. (2016), a similar trend in $\delta^{13}C_{Umed}$ is not recognizable for the Western Mediterranean Sea. This may express lower differences in the seasonal food supply between the sites or the in total higher input of organic matter compared to the Aegean Sea.

The $\delta^{13}C_{Umed}$ of unstained individuals from 5cm sediment depth in the western Mediterranean Sea and Strait of Sicily are on average 0.1 to 0.2‰ lower than those of stained specimens in the topmost centimeter. This adds to previous observations of Theodor et al. (2016) suggesting the influence of the Suess effect (Keeling, 1979; Quay et al., 1992) in living individuals while it is absent in sub-recent specimens. The Suess effect reduces $\delta^{13}C$ values in the atmosphere and oceans, due to the anthropogenic release of isotopically light CO_2 out of fossil fuels. A similar effect was not seen in the Aegean Sea since live and dead individuals were selected from the same sediment depth and thus had only minor age differences (Table 2, Fig.3). The only exception is Site 595 in the central Aegean Sea, where the deviation is even higher (0.5-0.7‰), when compared to the western Mediterranean Sea. Since this signal is

restricted to only one site it is probably due to relocation of fossil tests by the effects of bioturbation or lateral sediment transport.

Under well-oxygenated conditions, the pore water $\delta^{13}C_{DIC}$ gradient depends on the organic matter fluxes and associated decomposition rates of organic matter in the surface sediment (McCorkle and Emerson, 1988; McCorkle et al., 1985, 1990, Holsten et al., 2004). Organic matter fluxes also control the depth of the oxygenated layer (Rutgers van der Loeff, 1990) and thus the microhabitat range of infaunal foraminifera (Corliss, 1985; Jorissen et al, 1995; Koho et al., 2008; Koho & Pina–Ochoa, 2012). Subsurface waters in the Mediterranean Sea are well ventilated resulting in bottom water oxygen concentrations above 4.1ml l^{-1} at all sites in our study (MedAtlas, 1997). The $\delta^{13}C$ signal of *U. mediterranea* appears particularly suitable to monitor the pore water $\delta^{13}C_{DIC}$ signal in the surface-near sediment because it seems to be less influenced by species-specific "vital effects" (McConnaughy, 1989a; b) when compared to other shallow infaunal taxa, for example *U. peregrina* (Schmiedl et al., 2004; Theodor et al., 2016).

In this study, the deviation of $\delta^{13}C_{Umed}$ from bottom water $\delta^{13}C_{DIC}$ (reflected as higher $\Delta\delta^{13}C_{Umed\text{-}Epi}$ values, Fig. 4) suggests exponential relations with the MLD of *U. mediterranea*, the depth of the oxygenated layer and with the TOC content of the surface sediment. At the more oligotrophic to mesotrophic sites of the Mallorca Channel, the Gulf of Lions, the Spanish Slope off Barcelona, and the southern Aegean Sea, relatively low $\Delta\delta^{13}C_{Umed\text{-}Epi}$ values correspond to a relatively thick oxygenated layer and low TOC contents. The rather deep position of the redox boundary, exceeding 10cm at some sites, enables *U. mediterranea* to inhabit a relatively wide microhabitat range. In contrast relatively high $\Delta\delta^{13}C_{Umed\text{-}Epi}$ values at the more mesotrophic to eutrophic sites of the Alboran Sea coincide with relatively thin oxygenated layers and higher TOC contents. Here, the microhabitat range of *U. mediterranea* is compressed because of limited pore water oxygen (Fig. 4).

When comparing sites within the central and northern Aegean Sea, the foraminiferal stable isotope difference and the biogeochemical and ecological characteristics lack a consistent relation (Fig. 4). In these areas strongly negative $\Delta\delta^{13}C_{Umed\text{-}Epi}$ do not systematically

correspond to maximum TOC contents and the shallowest redox boundary (Fig. 4). The reasons for this absence of a clear relation between $\Delta\delta^{13}C_{Umed\text{-}Epi}$ and environmental parameters within this area cannot be unraveled with our data. It may be related to the high variability in oceanographic and biogeochemical conditions of the bottom water in the isolated basins that are characterized by focusing of organic-rich sedimentary material (Lykousis et al., 2002; Giresse et al., 2003; Poulos, 2009) and/or temporarily intermittent replenishment of deep waters on seasonal to decadal time scales (Zervakis et al., 2003; Velaoras & Lascaratos, 2005; Androulidakis et al., 2012). The first possibility can increase the supply of refractory C_{org}, recorded by higher TOC contents, and influence the foraminiferal microhabitat depths, but has minor effects on the $\delta^{13}C_{DIC}$ pore water gradient. Latter possibility refers to local ventilation events, which exchange aged bottom water with comparatively low $\delta^{13}C_{DIC}$ signature by surface waters enhanced in $^{13}C_{DIC}$. This may also push the pore water gradient towards stronger differences, explaining the more negative $\Delta\delta^{13}C_{Umed\text{-}Epi}$ values, compared to the remaining sites with similar conditions (Fig. 4).

4.3. Development of a stable carbon isotope based transfer function for organic carbon fluxes

Our results suggest a close relationship between the $\delta^{13}C$ gradient in pore waters of the surface sediment (expressed as $\Delta\delta^{13}C_{Umed\text{-}Epi}$) and the organic matter (OM) fluxes to the sea floor, for open-ocean settings of the western and central Mediterranean Sea and the southern Aegean Sea (Fig. 5). Based on these observations, we tested the potential for the development of a $\delta^{13}C$-based transfer function for OM flux rates. In open-ocean settings, the main food source of deep-sea environments is the exported OM from the surface layer, where photosynthetic primary production (PP) takes place (e.g. Boyd & Trull, 2007; Bishop, 2009). The majority of produced particulate organic carbon (POC) is recycled within the photic zone. In the open Mediterranean Sea, around 4% of the POC is exported out of the photic zone, which is lower than for other open oceans, caused by a specific nutrient distribution in the

405 Mediterranean Sea (Moutin & Raimbault, 2002; Gogou et al., 2014). The remineralization of
406 organic matter is intensified, which leads to reduced fluxes to the sea floor.

407 During transfer from the surface ocean to the deep-sea, the amount of exported OM
408 decreases exponentially reflecting microbial decay (Suess, 1980; de la Rocha & Passow,
409 2007; Packard & Gomez, 2013). Various functions have been developed for the estimation of
410 OM fluxes during sinking of particles through the water column integrating numerous
411 observational data (Suess, 1980; Betzer et al., 1984; Martin et al., 1987; Antia, et al., 2001).
412 The different functions reveal a high variability for the active surface layer, while the results for
413 deeper parts of the water column are within a comparable range (Felix, 2014). In our study
414 (Table 1, Fig.5), we applied the function of Betzer et al. (1984) for calculating the depth-
415 dependent C_{org} fluxes at the different Mediterranean sites using satellite-derived PP data
416 (Antoine & Morel, 1996; Uitz et al., 2008).

417 A comparison with direct PP and export flux measurements of sediment trap studies
418 revealed ambiguous results. The PP values calculated after Antoine and Morel (1996) are in a
419 comparable range to PP measurements in the western Mediterranean (Moutin & Raimbault,
420 2002; Sanchez–Vidal et al., 2004; 2005; Zúñiga et al., 2007, 2008). However, the estimated
421 export fluxes are too high in these areas compared to direct measurements of the referred
422 studies, probably due to the aforementioned high remineralization rate in the Mediterranean
423 Sea. However, the discrepancy in export fluxes is partly compensated by the application of the
424 21–30% lower PP values calculated after Uitz et al. (2008). For the Aegean Sea, in contrast,
425 distinctively higher measured PP values have been reported than were estimated (Siokou–
426 Frangou et al., 2002). For the Gulf of Lions measured OM export fluxes exceed the predicted
427 values (Heussner et al., 2006), which can be explained by the additional lateral input of organic
428 carbon channeled within the local canyon systems (Schmiedl et al., 2000). In order to
429 compensate for these possible additional C_{org} fluxes in marginal basin areas, the application
430 of the function of Antoine and Morel (1996) is more promising, hence a potential overestimation
431 of C_{org} fluxes in open-ocean areas has to be considered.

For both approaches of PP calculation (Antoine & Morel, 1996; Uitz et al., 2008) the relation between the estimated C_{org} fluxes and the $\Delta\delta^{13}C_{Umed\text{-}Epi}$ exhibits a complex pattern and at first instance lacks a simple and statistically significant correlation (Fig. 5). Particularly, strongly negative $\Delta\delta^{13}C_{Umed\text{-}Epi}$ in the central and northern Aegean Sea suggest high C_{org} fluxes, which however are not reflected in the estimated PP-based values. The eventual underestimation of C_{org} fluxes in these more marginal areas is likely caused by additional lateral OM input and the focusing of organic matter in isolated small basins. In fact, the northern and central Aegean Sea experiences high OM input from terrestrial sources through outflow of North Aegean rivers and the Black Sea (Aksu et al., 1999; Tsiaras et al., 2012). In contrast, the measured main redox boundary depth and the TOC contents do not indicate a higher supply in organic matter. However, sediment trap data from the northern Aegean Sea (Lykousis et al., 2002) reveal C_{org} fluxes of 35–81$gCm^{-2}a^{-1}$, which are 3 to 10 times higher than estimated values solely based on PP-based vertical fluxes. Although the high measured values can be partly attributed to the short sampling interval of two months in late spring and thus to elevated vertical fluxes during the spring bloom, elevated year-round lateral C_{org} fluxes can be expected, but of a clearly lower dimension. The measured ratio of primary to reworked OM in the sediment at this site is around 60–70% (Lykousis et al., 2002; Poulos, 2009), which leaves the PP as the main source of the C_{org} fluxes to the deep-sea. Similar results have been derived for canyon systems of the Gulf of Lions where OM resuspension, shelf to slope cascading and channeling results in significantly higher observed than PP-derived estimated C_{org} fluxes (Heussner et al., 2006; Pusceddu et al., 2010, Pasqual et al., 2010). Even in open slope settings, resuspended OM can significantly contribute to the total C_{org} flux (McCave et al., 2001; Tesi et al., 2010; Stabholz et al., 2013).

Despite these biases, it appears reasonable to develop a C_{org} flux transfer function at least for the more open marine settings of the western and central Mediterranean Sea and the southern Aegean Sea (Fig. 6). Here, vertical sinking of PP-derived OM appears to be the main source for C_{org} fluxes (Pusceddu et al., 2010) explaining the good correlation with the $\Delta\delta^{13}C_{Umed\text{-}Epi}$ values (Fig. 5). Elevated C_{org} fluxes of the upwelling-affected Alboran Sea

460 (Hernandez–Almeida et al., 2011) are reflected in rather negative $\Delta\delta^{13}C_{Umed\text{-}Epi}$ values while
461 the observed $\delta^{13}C$ differences in the more oligotrophic regions of the Mallorca Channel, the
462 Spanish Slope off Barcelona, the Strait of Sicily, and the southern Aegean Sea are lower. So,
463 omitting the data from the northern and central Aegean Sea, and considering sediment trap
464 data from the Gulf of Lions (Heussner et al., 2006) the derived function can be expressed as

465 $$C_{org}\ flux = -15.99 * \Delta\delta^{13}C_{Umed\text{-}Epi} + 0.34 \quad (1)$$

466 with a coefficient of determination (R^2) of 0.63 and a significance (p) of 0.0021 (Fig. 6). The
467 estimated C_{org} fluxes can be used to recalculate marine PP, but should be handled carefully,
468 due to the highly possible overestimation caused by lateral advection. Especially in more
469 marginal areas this bias can lead to unreliable recalculated PP values.

470 The application of this function to unstained *U. mediterranea* tests creates a higher
471 range of uncertainty. The main reason for this inconsistency seems to be the relocation of
472 fossil tests at particular sites, leading to significant contrasts between $\delta^{13}C_{Umed}$ values of
473 stained and unstained tests. For empty *U. mediterranea* tests, marked negative $\delta^{13}C_{Umed}$
474 outliers appear at Sites 537 and 396, which has already been mentioned in Theodor et al.
475 (2016) for the latter site. In the Alboran Sea (Sites 338 and 347) on the other hand, $\delta^{13}C_{Umed}$
476 values of unstained tests are about 0.50‰ higher than those of stained tests. Less distinct
477 $\delta^{13}C_{Umed}$ differences between autochthonous and allochthonous tests may not be detected so
478 easily. These potential uncertainties have to be considered in the application of the transfer
479 function to sediment cores, particularly to down-core records from sites influenced by strong
480 lateral transport such as Canyon environments or the Northern and Central Aegean Sea.
481 Likewise, the application of the transfer function to areas outside of the Mediterranean Sea
482 may be biased by contrasting remineralization rates, due to the specific oceanographic
483 conditions, especially the higher temperatures in the Mediterranean Sea. Further refinement
484 of this function will require an interdisciplinary effort including a larger number of direct C_{org}
485 flux measurements in sediment trap deployments, which can be directly related to the obtained
486 foraminiferal $\delta^{13}C$ signals.

5. Conclusions

The $\delta^{13}C$ signal of deep-sea benthic foraminifera from different areas of the western, central and eastern Mediterranean Sea reflects an integration of various environmental and biological signals. The application of epifaunal benthic foraminifera as an unbiased proxy for the $\delta^{13}C_{DIC}$ of the surrounding water mass is ambiguous, due to possible allochtonous tests, but also due to slight species-specific difference in the microhabitat that can result in significant $\delta^{13}C_{Epi}$ shifts. The $\delta^{13}C$ signal of the strictly epifaunal *Planulina ariminensis* should be preferred, in contrast to the $\delta^{13}C$ signal of the less strictly epifaunal *Cibicidoides pachydermus,* which appears to be influenced by pore water DIC and its $\delta^{13}C$ value.

The $\delta^{13}C$ signal of epifaunal taxa lacks ontogenetic effects supporting results from previous studies (Dunbar & Wefer, 1984; Corliss et al, 2002; Theodor et al., 2016). Significant ontogenetic effects were recorded in the $\delta^{13}C$ signal of *Uvigerina mediterranea*. While the ontogenetic increase of $\delta^{13}C_{Umed}$ is more or less comparable (0.11 ± 0.03‰ 100µm^{-1}) in the Western Mediterranean and the Strait of Sicily, a stronger increase and even a regional S-N trend is documented for the Aegean Sea (0.16 ± 0.04‰ 100µm^{-1}). In general, the $\delta^{13}C$ values of *U. mediterranea* from the Aegean Sea are more negative when compared to those from the western and central Mediterranean Sea. This regional contrast cannot be reconciled with different vital and pore water effects but instead seem to be caused by enhanced residence times of bottom waters in the partly isolated small basins within the Aegean Sea. In cases of well-oxygenated conditions the $\delta^{13}C_{Umed}$ signal, compared to bottom water, is mainly controlled by regional trophic contrasts and related remineralisation rates. The $\Delta\delta^{13}C_{Umed\text{-}Epi}$ are clearly related to the median microhabitat depth, the depth of the redox boundary (indicating the extent of the oxygenated layer), and to a lower extent to the TOC of the surface sediment. Based on satellite derived primary production estimates C_{org} fluxes were calculated and related to the recorded $\Delta\delta^{13}C_{Umed\text{-}Epi}$ values. Comparison with sediment trap data reveals underestimation of

satellite-derived C_{org} fluxes for the marginal areas of the central and northern Aegean Sea and the canyon systems of the Gulf of Lions. In these ecosystems additional lateral transport of resuspended and terrestrial OM contributes substantially to C_{org} fluxes. Considering these biases a first estimation for C_{org} fluxes in open-ocean settings of the Mediterranean Sea could be established.

Acknowledgements

We would like to thank K.-C. Emeis and two anonymous referees for their helpful remarks and suggestions. We thank the ship crews and scientists of R/V *Meteor* for good collaboration during cruises M40/4, M51/3, and M69/1. Thanks to Valerie Menke for foraminifera test size measurements and Mareike Paul for selection of epifaunal specimens. We thank David Antoine for suggestions on the GlobColour data set and Jürgen Möbius for support during processing of the TOC samples. Lisa Schönborn and Günther Meyer are thanked for technical support during stable isotope measurements. This study was supported by the Deutsche Forschungsgemeinschaft, grants SCHM1180/16 and MA1942/11.

Appendix A. List of benthic foraminiferal taxa used in this study.

Cibicides lobatulus (Walker & Jakob) = *Nautilus lobatulu*s Walker & Jacob, 1798, p. 642, pl. 14, fig. 36.

Cibicidoides pachydermus (Rzehak) = *Truncatulina pachyderma* Rzehak, 1886, p. 87, pl. 1, fig. 5.

Planulina ariminensis d'Orbigny = *Planulina ariminensis* d'Orbigny, 1826, p. 280, pl. 14, figs. 1–3.

Uvigerina mediterranea Hofker = *Uvigerina mediterranea* Hofker, 1932, p. 118–121, fig. 32.

References

Adkins, J.F., McIntyre, K., and Schrag, D.P.: The Salinity, Temperature, and δ18O of the Glacial Deep Ocean, Science, 298, 1769-1773, doi:10.1126/science.1076252, 2002.

Aksu, A.E., Abrajano, T., Mudie, P.J. and Yasar, D.: Organic geochemical and palynological evidence for terrigenous origin of the organic matter in Aegean sapropel S1. Mar. Geol., 153, 303-318, doi:10.1016/S0025-3227(98)00077-2, 1999.

Androulidakis, Y.S., Kourafalou, V.H., Kresenitis, Y.N., and Zervakis, V.: Variability of deep water mass characteristics in the North Aegean Sea: The role of lateral inputs and atmospheric conditions, Deep-Sea Res. Pt. I, 67, 55-72, doi:10.1016/j.dsr.2012.05.004, 2012.

Antia, A.N., Koeve,W., Fischer, G., Blanz, T., Schulz–Bull, D., Scholten, J., Neuer, S., Kremling, K., Kuss, J., Peinert, R., Hebbeln, D., Bathmann, U., Conte, M., Fehner, U. and Zeitzschel, B.: Basin-wide particulate carbon flux in the Atlantic Ocean: regional export patterns and potential for atmospheric CO2 sequestration, Global Biogeochem. Cy., 15, 845-862, doi: 10.1029/2000GB001376, 2001.

Antoine, D. and Morel, A.: Oceanic primary production: 1. Adaptation of a spectral light-photosynthesis model in view of application to satellite chlorophyll observations, Global Biogeochem. Cy., 10, 43-55, doi:10.1029/95GB02831, 1996.

Bemis, B.E., Spero, H.J., Bijma, J., and Lea, D.W.: Reevaluation of the oxygen isotopic composition of planktonic foraminifera: Experimental results and revised paleotemperature equations. Paleoceanography, 13(2), 150-160, doi:10.1029/98PA00070, 1998.

Bernhard, J.M.: Distinguishing Live from Dead Foraminifera: Methods Review and Proper Applications, Micropaleontology, 46, Supplement 1: Advances in the Biology of Foraminifera, 38-46, 2000.

Betzer, P.R., Showers, W.J., Laws, E.A., Winn, C.D., DiTullio, G.R., and Kroopnick, P.M.: Primary productivity and particle fluxes on a transect of the equator at 153°W in the Pacific Ocean, Deep-Sea Res., 31, 1-11, doi: 10.1016/0198-0149(84)90068-2, 1984.

Bishop, J.K.B.: Autonomous observations of the ocean biological carbon pump, Oceanography, 22, 182-193, doi:10.5670/oceanog.2009.48, 2009.

568 Bosc, E., Bricaud, A., and Antoine, D., 2004. Seasonal and interannual variability in algal
569 biomass and primary production in the Mediterranean Sea, as derived from 4 years of
570 SeaWiFS observations. Global Biogeochemical Cycles 18, GB1005,
571 doi:10.1029/2003GB002034, 2004
572 Boyd, P.W. and Trull, T.W.: Understanding the export of biogenic particles in oceanic waters:
573 Is there consensus?, Prog. Oceanogr., 72, 276-312, doi:10.1016/j.pocean.2006.10.007,
574 2007.
575 Brückner, S. and Mackensen, A.: Organic matter rain rates, oxygen availability, and vital effects
576 from benthic foraminiferal δ13C in the historic Skagerrak, North Sea, Mar. Micropaleontol.,
577 66, 192-207, doi:10.1016/j.marmicro.2007.09.002, 2008.
578 Canals, M., Company, J.B., Martín, D., Sànchez–Vidal, A., and Ramírez–Llodrà, E.: Integrated
579 study of Mediterranean deep canyons: Novel results and future challenges, Prog.
580 Oceanogr. 118, 1-27, doi:10.1016/j.pocean.2013.09.004, 2013.
581 Corliss, B.H.: Microhabitats of benthic foraminifera within deep-sea sediments, Nature, 314,
582 435-438, doi:10.1038/314435a0, 1985.
583 Corliss, B.H., McCorkle, D.C., and Higdon, D.M.: A time series study of the carbon isotopic
584 composition of deep-sea benthic foraminifera, Paleoceanography, 17, 1036,
585 doi:10.1029/2001PA000664, 2002.
586 Curry, W.B. and Lohmann, G.P.: Carbon Isotopic Changes in Benthic Foraminifera from the
587 Western South Atlantic: Reconstruction of Glacial Abyssal Circulation Patterns, Quaternary
588 Res., 18, 218-235, doi:10.1016/0033-5894(82)90071-0, 1982.
589 Danovaro, R., Dinet, A., Duineveld, G., and Tselepides, A.: Benthic response to particulate
590 fluxes in different trophic environments: a comparison between the Gulf of Lions–Catalan
591 Sea (western-Mediterranean) and the Cretan Sea (eastern-Mediterranean), Prog.
592 Oceanogr., 44, 287-312, doi:10.1016/S0079-6611(99)00030-0, 1999.
593 De La Rocha, C. and Passow, U., Factors influencing the sinking of POC and the efficiency of
594 the biological carbon pump, Deep-Sea Res. Pt. II, 54, 639-658,
595 doi:10.1016/j.dsr2.2007.01.004, 2007.

596 Dunbar, R.B., and Wefer, G.: Stable isotope fractionation in benthic foraminifera from the
597 Peruvian continental margin. Mar. Geol., 59, 215-225, doi:10.1016/0025-3227(84)90094-X
598 1984.
599 Edgar, K.M., Pälike, H., and Wilson, P.A.: Testing the impact of diagenesis on the δ18O and
600 δ13C of benthic foraminiferal calcite from a sediment burial depth transect in the equatorial
601 Pacific, Paleoceanography, 28, 468-480, doi:10.1002/palo.20045, 2013.
602 Felix, M.: A comparison of equations commonly used to calculate organic carbon content and
603 marine palaeoproductivity from sediment data, Mar. Geol., 347, 1-11,
604 doi:10.1016/j.margeo.2013.10.006, 2014.
605 Fontanier, C., Mackensen, A., Jorissen, F.J., Anschutz, P., Licari, L., and Griveau, C.: Stable
606 oxygen and carbon isotopes of live benthic foraminifera from the Bay of Biscay: Microhabitat
607 impact and seasonal variability, Mar. Micropaleontol., 58, 159-183,
608 doi:10.1016/j.marmicro.2005.09.004, 2006.
609 Franco–Fraguas, P., Badaraco Costa, K., and de Lima Toledo, F. A.: Stable Isotope/Test size
610 relationship in Cibicidoides wuellerstorfi, Braz. J. Oceanogr., 59, 287-291,
611 doi:10.1590/S1679-87592011000300010, 2011.
612 Giresse, P., Buscail, R., and Charrière, B.: Late Holocene multisource material input into the
613 Aegean Sea: depositional and post-depositional processes, Oceanol. Acta, 26, 657-672,
614 doi: 10.1016/j.oceact.2003.09.001, 2003.
615 Gogou, A., Sanchez–Vidal, A., Durrieu de Madron, X., Stavrakakis, S., Calafat, A.M., Stabholz,
616 M., Psarra, S., Canals, M., Heussner, S., Stavrakaki, I., and Papathanassiou, E.: Carbon
617 flux to the deep in three open sites of the Southern European Seas (SES), J. Mar. Syst.,
618 129, 224-233, doi:10.1016/j.jmarsys.2013.05.013, 2014.
619 Grossman, E. L.,: Carbon isotopic fractionation in live benthic foraminifera – comparison with
620 inorganic precipitate studies, Geochim. Cosmochim. Acta, 48, 1505-1512,
621 doi:10.1016/0016-7037(84)90406-X, 1984a.

622 Grossman, E. L.,: Stable isotope fractionation in live benthic Foraminifera from the Southern
623 California Borderland, Palaeogeogr. Palaeoclimatol. Palaeoecol., 47, 301-327,
624 doi:10.1016/0031-0182(84)90100-7, 1984b.
625 Hemleben, C., Becker, T., Bellas, S., Benningsen, G., Casford, J., Cagatay, N., Emeis, K.-C.,
626 Engelen, B., Ertan, T., Fontanier, C., Friedrich, O., Frydas, D., Giunta, S., Hoffelner, H.,
627 Jorissen, F., Kahl, G., Kaszemeik, K., Lykousis, V., Meier, S., Nickel, G., Overman, J.,
628 Pross, J., Reichel, T., Robert, C., Rohling, E., Ruschmeier, W., Sakinc, M., Schiebel, R.,
629 Schmiedl, G., Schubert, K., Schulz, H., Tischnak, J., Truscheit, T.: Ostatlantik – Mittelmeer
630 - Schwarzes Meer, Part 3, Cruise No.51, Leg 3, 14 November – 10 December 2001, Valetta
631 – Istanbul. METEOR-Berichte, Universität Hamburg, 03-1, 57 pp., 2003.
632 Hernández–Almeida, I. Bárcena, M.A., Flores, J.A., Sierro, F.J., Sanchez–Vidal, A., Calafat,
633 A.: Microplankton response to environmental conditions in the Alboran Sea (Western
634 Mediterranean): One year sediment trap record. Mar. Micropaleontol., 78, 14-24,
635 doi:10.1016/j.marmicro.2010.09.005, 2011.
636 Heussner, S., Durrieu de Madron, X., Calafat, A., Canals, M., Carbonne, J., Delsaut, N., and
637 Saragoni, G.: Spatial and temporal variability of downward particle fluxes on a continental
638 slope: Lessons from an 8-yr experiment in the Gulf of Lions (NW Mediterranean), Mar.
639 Geol., 234, 63-92, doi:10.1016/j.margeo.2006.09.003, 2006.
640 Hieke, W., Hemleben, C., Linke, P., Türkay, M., Weikert, H.: Mittelmeer 1998/99, Cruise No.40,
641 28 October 1997 – 10 February 1998. METEOR-Berichte, Universität Hamburg, 99-2, 286
642 pp., 1999.
643 Holsten, J., Stott, L., and Berelson, W.: Reconstructing benthic carbon oxidation rates using
644 δ13C of benthic foraminifera, Mar. Micropaleontol., 53, 117-132, doi:
645 doi:10.1016/j.marmicro.2004.05.006, 2004.
646 Hoogakker, B.A.A., Elderfield, H., Schmiedl, G., McCave, I.N., and Rickaby, R.E.M.: Glacial-
647 interglacial changes in bottom-water oxygen content on the Portuguese margin, Nat.
648 Geosci., 8, 40-43, doi:10.1038/NGEO2317, 2015.

649 Hübscher, C., Betzler, C., Grevemeyer, I.: Sedimentology, rift-processes and neotectonic in
650 the western Mediterranean, Cruise No. 69, 08 August – 20 September 2006, Las Palmas
651 (Spain) – Cartagena (Spain) – La Valletta (Malta). METEOR-Berichte, Universität Hamburg,
652 99-2, 86 pp., 2010.
653 Huertas, I. E., Rios, A. F., Garcia–Lafuente, J., Navarro, G., Makaoui, A., Sanchez–Roman,
654 A., Rodriguez–Galvez, S., Orbi, A., Ruiz, J., and Perez, F. F.: Atlantic forcing of the
655 Mediterranean oligotrophy, Global Biogeochem. Cycles, 26, Gb2022,
656 doi:10.1029/2011gb004167, 2012.
657 Jorissen, F.J., de Stigter, H.C., and Widmark, J.G.V.: A conceptual model explaining benthic
658 foraminiferal microhabitats, Mar. Micropaleontol., 26, 3-15, doi:10.1016/0377-
659 8398(95)00047-X, 1995.
660 Keeling, C.D.: The Suess effect: 13Carbon-14Carbon interrelations, Environ. Int., 2, 229-300,
661 doi:10.1016/0160-4120(79)90005-9, 1979.
662 Kitazato, H.: Foraminiferal microhabitats in four marine environments around Japan, Mar.
663 Micropaleontol., 24, 29-41, doi:10.1016/0377-8398(94)90009-4, 1994.
664 Koho, K.A., García, R., de Stigter, H.C., Epping, E., Koning, E., Kouwenhoven, T.J., and van
665 der Zwaan, G.J.: Sedimentary labile organic carbon and pore water redox control on
666 species distribution of benthic foraminifera: A case study from Lisbon–Setúbal Canyon
667 (southern Portugal), Prog. Oceanogr., 79, 55-82, doi:10.1016/j.pocean.2008.07.004, 2008.
668 Koho, K.A. and Piña–Ochoa, E.: Benthic Foraminifera: Inhabitants of low-oxygen
669 environments, in: Altenbach, A.V., Bernhard, J.M., and Seckbach, J. (Eds.): Anoxia:
670 Evidence for Eukaryote Survival and Paleontological Strategies, Cellular Origin, Life in
671 Extreme Habitats and Astrobiology, 21, 249–285, doi:10.1007/978-94-007-1896-8_14,
672 2012.
673 Kuhnt, T., Schmiedl, G., Ehrmann, W., Hamann, Y., and Andersen, N.: Stable isotope
674 composition of Holocene benthic foraminifers from the Eastern Mediterranean Sea: Past
675 changes in productivity and deep water oxygenation. Palaeogeogr., Palaeoclimatol.,
676 Palaeoecol., 268, 106-115, doi:10.1016/j.palaeo.2008.07.010, 2008.

677 Lascaratos, A., Roether, W., Nittis, K., and Klein, B.: Recent changes in the Eastern
678 Mediterranean Deep Waters: a review, Prog. Oceanogr., 44, 5-36, doi:10.1016/S0079-
679 6611(99)00019-1, 1999.
680 Licari, L. and Mackensen, A.: Benthic foraminifera off West Africa (1°N to 32°S): Do live
681 assemblages from the topmost sediment reliably record environmental variability?, Mar.
682 Micropaleontol., 55, 205-233, doi:10.1016/j.marmicro.2005.03.001, 2005.
683 Linke, P. and Lutze, G.F.: Microhabitat preferences of benthic foraminifera a static concept or
684 a dynamic adaptation to optimize food acquisition?, Mar. Micropaleontol., 20, 215-234,
685 doi:10.1016/0377-8398(93)90034-U, 1993.
686 López–Sandoval, D. C., Fernández, A., and Marañón, E.: Dissolved and particulate primary
687 production along a longitudinal gradient in the Mediterranean Sea, Biogeosciences, 8, 815-
688 825, doi:10.5194/bg-8-815-2011, 2011.
689 Lutze, G.F. and Thiel, H.: Epibenthic foraminifera from elevated microhabitats: Cibicidoides
690 wuellerstorfi and Planulina ariminensis, J. Foramin. Res., 19, 153-158,doi:
691 10.2113/gsjfr.19.2.153, 1989.
692 Lykousis, V., Chronis, G., Tselepides, A., Price, B., Theocharis, A., Siokou–Frangou, I., Van
693 Wambeke, F., Danovaro, R., Stavrakakis, S., Duineveld, G., Georgopoulos, D., Ignatiades,
694 L., Souvermezoglou, E., and Voutsinou–Taliadouri, F.: Major outputs of the recent
695 multidisciplinary biogeochemical researches undertaken in the Aegean Sea, J. Marine
696 Syst., 33–34, 313–334, doi:10.1016/S0924-7963(02)00064-7, 2002.
697 Lyle, M.: The brown-green color transition in marine sediments: A marker of the Fe(III)-Fe(II)
698 redox boundary. Limnol. Oceanogr., 28, 1026-1033, doi:10.4319/lo.1983.28.5.1026, 1983.
699 Mackensen, A.: On the use of benthic foraminiferal δ13C in palaeoceanography: constraints
700 from primary proxy relationships, in: Austin, W.E.N. and James, R.H. (eds.):
701 Biogeochemical Controls on Palaeoceanographic Environmental Proxies, Geological
702 Society, London, Special Publications 303, pp. 121–133, doi:10.1144/SP303.9, 2008.
703 Mackensen, A., and Bickert, T.: Stable carbon isotopes in benthic foraminifera: Proxies for
704 deep and bottom water circulation and new production. In: Fischer, G., and Wefer, G. (Eds.),

705 Use of proxies in paleoceanography: Examples from the South Atlantic. Springer, Berlin,
706 Heidelberg, pp. 229-254, doi:10.1007/978-3-642-58646-0_9, 1999.
707 Mackensen, A., and Douglas, R.G.: Down-core distribution of live and dead deep-water benthic
708 foraminifera in box cores from the Weddell Sea and the California continental borderland,
709 Deep-Sea Res., 36, 879-900, doi:10.1016/0198-0149(89)90034-4, 1989.
710 Mackensen, A., and Licari, L.: Carbon isotopes of live benthic foraminifera from the eastern
711 South Atlantic Ocean: Sensitivity to organic matter rain rates and bottom water carbonate
712 saturation state. In: Wefer, G., Mulitza, S., and Rathmeyer, V. (Eds.), The South Atlantic in
713 the Late Quaternary - Reconstruction of material budget and current systems. Springer-
714 Verlag, Berlin, pp. 623-644, doi:10.1007/978-3-642-18917-3_27, 2004.
715 Mackensen, A., Schumacher, S., Radke, J., and Schmidt, D.N.: Microhabitat preferences and
716 stable carbon isotopes of endobenthic foraminifera: clue to quantitative reconstruction of
717 oceanic new production?, Mar. Micropaleontol., 40, 233-258, doi:10.1016/S0377-
718 8398(00)00040-2, 2000.
719 Marchitto, T.M., Curry, W.B., Lynch-Stieglitz, J., Bryan, S.P., Cobb, K.M., and Lund, D.C.:
720 Improved oxygen isotope temperature calibrations for cosmopolitan benthic foraminifera,
721 Geochimica et Cosmochimica Acta, 130, 1–11, doi:10.1016/j.gca.2013.12.034, 2014.
722 Martin, J.H., Knauer, G.A., Karl, D.M., and Broenkow, W.W.: VERTEX: carbon cycling in the
723 northeast Pacific, Deep-Sea Res., 34, 267-285, doi:10.1016/0198-0149(87)90086-0, 1987.
724 McCave, I.N., Hall, I.R., Antia, A.N., Chou, L., Dehairs, F., Lampitt, R.S., Thomsen, L., van
725 Weering, T.C.E., and Wollast, R.: Distribution, composition and flux of particulate material
726 over the European margin at 47°–50°N, Deep-Sea Res. Pt. II, 48, 3107–3139,
727 doi:10.1016/S0967-0645(01)00034-0, 2001.
728 McConnaughey T.: 13C and 18O isotopic disequilibrium in biological carbonates: I. Patterns,
729 Geochim. Cosmochim. Acta, 53, 151-162, doi:10.1016/0016-7037(89)90282-2, 1989a.
730 McConnaughey T. 13C and 18O isotopic disequilibrium in biological carbonates: II. in vitro
731 simulation of kinetic isotope effects, Geochim. Cosmochim. Acta, 53, 163-171,
732 doi:10.1016/0016-7037(89)90283-4, 1989b.

McCorkle, D.C. and Emerson, S.R.: The relationship between pore water carbon isotopic composition and bottom water oxygen concentration, Geochim. Cosmochim. Acta, 52, 1169-1178, doi:10.1016/0016-7037(88)90270-0, 1988.

McCorkle, D.C., Bernhard, J.M., Hintz, C.J., Blanks, J.K., Chandler, G.T., and Shaw, T.J.: The carbon and oxygen stable isotopic composition of cultured benthic foraminifera, in: Austin, W.E.N. and James, R.H. (eds.): Biogeochemical Controls on Palaeoceanographic Environmental Proxies, Geological Society, London, Special Publications 303, 135-154, doi:10.1144/SP303.10, 2008.

McCorkle, D.C., Corliss, B.H., and Farnham, C.A.: Vertical distributions and stable isotopic compositions of live (stained) benthic foraminifera from the North Carolina and California continental margins, Deep-Sea Res. Pt. I, 44, 983-1024, doi:10.1016/S0967-0637(97)00004-6, 1997.

McCorkle, D.C., Emerson, S.R., and Quay, P.D.: Stable carbon isotopes in marine porewaters, Earth Planet. Sc. Lett., 74, 13-26, doi:10.1016/0012-821X(85)90162-1, 1985.

McCorkle, D.C., Keigwin, L.D., Corliss, B.H., and Emerson, S.R.: The influence of microhabitats on the carbon isotopic composition of deep-sea benthic foraminifera, Paleoceanography, 5, 161-185, doi:10.1029/PA005i003p00295, 1990.

MedAtlas, 1997. Mediterranean Hydrographic Atlas (Mast Supporting Initiative; MAS2-CT93-0074): CD-ROM.

Möbius, J., Lahajnar, N., and Emeis, K.-C.: Diagenetic control of nitrogen isotope ratios in Holocene sapropels and recent sediments from the Eastern Mediterranean Sea, Biogeosciences, 7, 3901-3914, doi:10.5194/bg-7-3901-2010, 2010a.

Möbius, J Lahajnar, N., and Emeis, K.-C.: Chemical composition of surface sediment samples from the Eastern Mediterranean Sea. doi:10.1594/PANGAEA.754732, 2010b.

Moutin, T. and Raimbault, P.: Primary production, carbon export and nutrients availability in western and eastern Mediterranean Sea in early summer 1996 (MINOS cruise), J. Marine Syst., 33-34, 273-288, doi: 10.1016/S0924-7963(02)00062-3, 2002.

760 Ohga, T. and Kitazato, H.: Seasonal changes in bathyal foraminiferal populations in response
761 to the flux of organic matter (Sagami Bay, Japan), Terra Nova, 9, 33-37, doi:10.1046/j.1365-
762 3121.1997.d01-6.x, 1997.
763 Packard, T.T. and Gómez, M.: Modeling vertical carbon flux from zooplankton respiration,
764 Prog. Oceanogr., 110, 59-68, doi:10.1016/j.pocean.2013.01.003, 2013.
765 Pahnke, K., and Zahn, R.: Southern hemisphere water mass conversion with North Atlantic
766 climate variability. Science, 307, 1741-1746, doi:10.1126/science.1102163, 2005.
767 Pasqual, C., Sanchez–Vidal, A., Zúñiga, D., Calafat, A., Canals, M., Durrieu de Madron, X.,
768 Puig, P., Heussner, S., Palanques, A., and Delsaut, N.: Flux and composition of settling
769 particles across the continental margin of the Gulf of Lion: the role of dense shelf water
770 cascading, Biogeosciences, 7, 217-231, doi:10.5194/bg-7-217-2010, 2010.
771 Pierre, C.: The oxygen and carbon isotope distribution in the Mediterranean water masses,
772 Mar. Geol., 153, 41-55, doi:10.1016/S0025-3227(98)00090-5, 1999.
773 Pinardi, N. and Masetti, E.: Variability of the large scale general circulation of the
774 Mediterranean Sea from observations and modelling: a review, Palaeogeogr.
775 Palaeoclimatol. Palaeoecol., 158, 153-173, doi:10.1016/S0031-0182(00)00048-1, 2000.
776 Pinardi, N., Zavatarelli, M., Adani, M., Coppini, G., Fratianni, C., Oddo, P., Simoncelli, S.,
777 Tonani, M, Lyubartsev, V., Dobricic, S. and Bonaduce, A.: Mediterranean Sea large-scale
778 low-frequency ocean variability and water mass formation rates from 1987 to 2007: A
779 retrospective analysis, Prog. Oceanogr. 132, 318-332, doi:10.1016/j.pocean.2013.11.003,
780 2015.
781 Poulos, S.E.: Origin and distribution of the terrigenous component of the unconsolidated
782 surface sediment of the Aegean floor: A synthesis, Cont. Shelf Res., 29, 2045–2060,
783 doi:10.1016/j.csr.2008.11.010, 2009.
784 Puig, P. and Palanques. A.: Temporal variability and composition of settling particle fluxes on
785 the Barcelona continental margin (Northwestern Mediterranean), J. Mar. Res., 56, 639-654,
786 doi:10.1357/002224098765213612, 1998.

787 Pujo–Pay, M., Conan, P., Oriol, L., Cornet–Barthaux, V., Falco, C., Ghiglione, J.-F., Goyet, C.,
788 Moutin, T., and Prieur, L.: Integrated survey of elemental stoichiometry (C,N,P) from the
789 western to eastern Mediterranean Sea, Biogeosciences, 8, 883-899, doi:10.5194/bg-8-883-
790 2011, 2011.
791 Pusceddu, A., Bianchelli, S., Canals, M., Sanchez–Vidal, A., Durrieu de Madron, X., Heussner,
792 S., Lykousis, V., de Stigter, H., Trincardi, F., and Danovaro, R.: Organic matter in sediments
793 of canyons and open slopes of the Portuguese, Catalan, Southern Adriatic and Cretan Sea
794 margins, Deep-Sea Res. Pt. I, 57, 441–457, doi:10.1016/j.dsr.2009.11.008, 2010a.
795 Quay, P.D., Tilbrook, B., and Wong, C.S.: Oceanic Uptake of Fossil Fuel CO2: Carbon-13
796 Evidence, Science, 256, 74-79, doi: 10.1126/science.256.5053.74, 1992.
797 Rathburn, A.E. and Corliss, B.H.: The ecology of living (stained) deep-sea benthic foraminifera
798 from the Sulu Sea, Paleoceanography, 9, 87-150, doi: 10.1029/93PA02327, 1994.
799 Rathburn, A.E., Corliss, B.H., Tappa, K.D., and Lohmann, K.C.: Comparisons of the ecology
800 and stable isotopic compositions of living (stained) benthic foraminifera from the Sulu and
801 South China Seas, Deep-Sea Res. Pt. I, 43, 1617-1646, doi:10.1016/S0967-
802 0637(96)00071-4, 1996.
803 Rhein, M., Send, U., Klein, B., and Krahmann, G.: Interbasin deep water exchange in the
804 western Mediterranean. J. Geophys. Res. 104 (C10), 23,495–23,508,
805 doi:10.1029/1999JC900162, 1999.
806 Roether, W., Manca, B. B., Klein, B., Bregant, D., Georgopoulos, D., Beitzel, V., Kovacevic,
807 V., and Luchetta, A.: Recent changes in eastern Mediterranean deep waters, Science, 271,
808 333-335, doi: 10.1126/science.271.5247.333, 1996.
809 Roether, W., Klein, B., Manca, B.B., Theocharis, A., and Kioroglou, S.: Transient Eastern
810 Mediterranean deep waters in response to the massive dense-water output of the Aegean
811 Sea in the 1990s, Prog. Oceanogr., 74, 540-571., doi:10.1016/j.pocean.2007.03.001, 2007.
812 Rutgers van der Loeff, M.M.: Oxygen in pore waters of deep-sea sediments, Philos. Trans. R.
813 Soc. London, Ser. A, 331, 69-84, doi: 10.1098/rsta.1990.0057, 1990.

814 Sanchez–Vidal, A., Calafat, A., Canals, M., and Fabres, J.: Particle fluxes in the Almeria-Oran
815 Front: control by coastal upwelling and sea surface circulation, J. Mar. Syst., 52, 89-106,
816 doi:10.1016/j.jmarsys.2004.01.010, 2004.
817 Sanchez–Vidal, A., Calafat, A., Canals, M., Frigola, J., and Fabres, J.: Particle fluxes and
818 organic carbon balance across the Eastern Alboran Sea (SW Mediterranean Sea), Cont.
819 Shelf Res., 25, 609-628, doi:10.1016/j.csr.2004.11.004, 2005.
820 Send, U., Font, J., Krahmann, G., Millot, C., Rhein, M., and Tintore, J.: Recent advances in
821 observing the physical oceanography of the western Mediterranean Sea. Prog. Oceanogr.
822 44, 37–64, doi:10.1016/S0079-6611(99)00020-8, 1999.
823 Schilman, B., Almogi–Labin, A., Bar–Matthews, M., and Luz, B.: Late Holocene productivity
824 and hydrographic variability in the eastern Mediterranean inferred from benthic foraminiferal
825 stable isotopes. Paleoceanography, 18, doi:10.1029/2002PA000813, 2003.
826 Schmiedl, G. and Mackensen, A.: Multispecies stable isotopes of benthic foraminifers reveal
827 past changes of organic matter decomposition and deepwater oxygenation in the Arabian
828 Sea, Paleoceanography, 21, PA4213, doi:10.1029/2006PA001284, 2006.
829 Schmiedl, G., de Bovée, F., Buscail, R., Charrière, B., Hemleben, C., Medernach, L., and
830 Picon, P.: Trophic control of benthic foraminiferal abundance and microhabitat in the bathyal
831 Gulf of Lions, western Mediterranean Sea, Mar. Micropaleontol., 40, 167-188,
832 doi:10.1016/S0377-8398(00)00038-4, 2000.
833 Schmiedl, G., Pfeilsticker, M., Hemleben, C., and Mackensen, A.: Environmental and biological
834 effects on the stable isotope composition of recent deep-sea benthic foraminifera from the
835 western Mediterranean Sea, Mar. Micropaleontol., 51, 129-152,
836 doi:10.1016/j.marmicro.2003.10.001, 2004.
837 Schroeder, K., Gasparini, G. P., Tangherlini, M., and Astraldi, M.: Deep and intermediate water
838 in the Western Mediterranean under the influence of the Eastern Mediterranean Transient,
839 Geophys. Res. Lett., 33, L21607, doi:10.1029/2006GL027121, 2006.

840 Schroeder, K., Ribotti, A., Borghini, M., Sorgente, R., Perilli, A., and Gasparini, G. P.: An
841 extensive western Mediterranean deep water renewal between 2004 and 2006, Geophys.
842 Res. Lett., 35, L18605, doi:10.1029/2008GL035146, 2008.
843 Schumacher, S., Jorissen, F.J., Mackensen, A., Gooday, A.J., and Pays, O.: Ontogenetic
844 effects on stable carbon and oxygen isotopes in tests of live (Rose Bengal stained) benthic
845 foraminifera from the Pakistan continental margin, Mar. Micropaleontol., 76, 92-103,
846 doi:10.1016/j.marmicro.2010.06.002, 2010.
847 Shackleton, N.J. and Opdyke, N.D.: Oxygen Isotope and Palaeomagnetic Stratigraphy of
848 Equatorial Pacific Core V28-238: Oxygen Isotope Temperatures and Ice Volumes on a 105
849 Year and 106 Year Scale, Quat. Res., 3, 39-55, doi:10.1016/0033-5894(73)90052-5, 1973.
850 Siokou–Frangou, I., Bianchi, M., Christaki, U., Christou, E. D., Giannakourou, A., Gotsis, O.,
851 Ignatiades, L., Pagou, K., Pitta, P., Psarra, S., Souvermezoglou, E., Van Wambeke, F., and
852 Zervakis, V.: Carbon flow in the planktonic food web along a gradient of oligotrophy in the
853 Aegean Sea (Mediterranean Sea), J. Mar. Syst., 33-34, 335-353, doi:10.1016/S0924-
854 7963(02)00065-9, 2002.
855 Skliris, N., Mantziafou, A., Sofianos, S., and Gkanaos, A.: Satellite-derived variability of the
856 Aegean Sea ecohydrodynamics, Cont. Shelf Res. 30, 403-418,
857 doi:10.1016/j.csr.2009.12.012, 2010.
858 Stabholz, M., Durrieu de Madron, X., Canals, M., Khripounoff, A., Taupier–Letage, I., Testor,
859 P., Heussner, S., Kerhervé, P., Delsaut, N.,. Houpert, L, Lastras, G., and Dennielou, B.:
860 Impact of open-ocean convection on particle fluxes and sediment dynamics in the deep
861 margin of the Gulf of Lions, Biogeosciences, 10, 1097-1116, doi:10.5194/bg-10-1097-2013,
862 2013.
863 Stott, L.D., Berelson, W., Douglas, R., and Gorsline, D., 2000. Increased dissolved oxygen in
864 Pacific intermediate waters due to lower rates of carbon oxidation in sediments. Nature,
865 407, 367-370, doi:10.1038/35030084, 2000.
866 Suess, E.: Particulate organic carbon flux in the oceans - surface productivity and oxygen
867 utilization, Nature, 288, 260–263, doi:10.1038/288260a0, 1980.

868 Tanhua, T., Hainbucher, D., Schroeder, K., Cardin, V., Álvarez, M., and Civitarese, G.: The
869 Mediterranean Sea system: a review and an introduction to the special issue, Ocean Sci.,
870 9, 789-803, doi:10.5194/os-9-789-2013, 2013.

871 Tesi, T., Puig, P., Palanques, A., and Goñi, M.A.: Lateral advection of organic matter in
872 cascading-dominated submarine canyons, Prog. Oceanogr., 84, 185-203,
873 doi:10.1016/j.pocean.2009.10.004, 2010.

874 Theodor, M., Schmiedl, G., and Mackensen, A.: Stable isotope composition of deep-sea
875 benthic foraminifera under contrasting trophic conditions in the western Mediterranean Sea,
876 Mar. Micropaleontol., 124, 16-28, doi:10.1016/j.marmicro.2016.02.001, 2016.

877 Tsiaras, K.P., Kourafalou, V.H., Raitsos, D.E., Triantafyllou, G., Petihakis, G., and Korres, G.:
878 Inter-annual productivity variability in the North Aegean Sea: Influence of thermohaline
879 circulation during the Eastern Mediterranean Transient, J. Mar. Syst., 96-97, 72-81,
880 doi:10.1016/j.jmarsys.2012.02.003, 2012.

881 Uitz, J., Huot, Y., Bruyant, F., Babin, M., and Claustre, H.: Relating phytoplankton
882 photophysiological properties to community structure on large scales, Limnol. Oceanogr.,
883 53, 614-630, doi:10.4319/ lo.2008.53.2.0614, 2008.

884 Velaoras, D. and Lascaratos, A.: Deep water mass characteristics and interannual variability
885 in the North and Central Aegean Sea, J. Mar. Syst., 53, 59-85,
886 doi:10.1016/j.jmarsys.2004.05.027, 2005.

887 Walton, W.R.: Techniques for recognition of living foraminifera, Contributions from the
888 Cushman Foundation for Foraminiferal Research, 3, 56-60, 1952.

889 Wüst, G.: On the vertical circulation of the Mediterranean Sea. J. Geophys. Res. 66, 3261–
890 3271, doi:10.1029/JZ066i010p03261, 1961.

891 Zahn, R., Winn, K., and Sarnthein, M.: Benthic Foraminiferal $\delta^{13}C$ and accumulation rates of
892 organic Carbon: Uvigerina peregrina group and Cibicidoides wuellerstorfi,
893 Paleoceanography, 1, 27-42, doi:10.1029/PA001i001p00027, 1986.

894 Zervakis, V., Krasakopoulou, E., Georgopoulos, D., and Souvermezoglou, E.: Vertical diffusion
895 and oxygen consumption during stagnation periods in the deep North Aegean, Deep-Sea
896 Res. Pt. I, 50, 53-71, doi:10.1016/S0967-0637(02)00144-9, 2003.
897 Zúñiga, D., Calafat, A., Sanchez–Vidal, A., Canals, M., Price, B., Heussner, S., and Miserocchi,
898 S.: Particulate organic carbon budget in the open Algero-Balearic Basin (Western
899 Mediterranean): Assessment from a one-year sediment trap experiment, Deep-Sea Res.
900 Pt. I, 54, 1530-1548, doi:10.1016/j.dsr.2007.06.001, 2007.
901 Zúñiga, D., Calafat, A., Heussner, S., Miserocchi, S., Sanchez–Vidal, A., Garcia–Orellana, J.,
902 Canals, M., Sánchez–Cabeza, J.A., Carbonne, J., Delsaut, N., Saragoni, G.: Compositional
903 and temporal evolution of particle fluxes in the open Algero–Balearic basin (Western
904 Mediterranean), J. Mar. Syst., 70, 196-214, doi:10.1016/j.jmarsys.2007.05.007, 2008.
905

Table captions

Table 1. Position, water depth, median living depth (MLD) of *Uvigerina mediterranea*, geochemical, Primary Production (PP) and C_{org} flux values of the investigated multicorer sites. Annual PP values are averages for the year previous to sampling after data from the GlobColour project. C_{org} fluxes were calculated after Betzer et al. (1984) and the MLD after Theodor et al. (2016). Data of the Canyon and Slope Sites were taken from Schmiedl et al. (2004).

Table 2. Average stable carbon isotope composition of selected benthic foraminifera with standard deviations. Underlined values of epifaunal species were applied to estimate $\delta^{13}C_{Epi}$. Also given are values for *Uvigerina mediterranea* tests larger than 600µm and the difference of this species compared to the average epifaunal stable carbon isotope ratios ($\Delta\delta^{13}C_{Umed\text{-}Epi}$).

Table 3. Linear regressions of ontogenetic trends of $\delta^{13}C_{Umed}$. The measured number of stained and unstained tests as well as the significance values are added.

921 Table 1.

Site	latitude	longitude	station depth (m)	MLD_{Umed} (cm)	redox boundary depth (cm)	TOC (%)	PP (Antoine & Morel, 1996) ($gCm^{-2}a^{-1}$)	PP (Uitz et al., 2008) ($gCm^{-2}a^{-1}$)	C_{org} flux (Antoine & Morel, 1996) ($gCm^{-2}a^{-1}$)	C_{org} flux (Uitz et al., 2008) ($gCm^{-2}a^{-1}$)
537	37°02.14‘ N	13°11.35‘ E	472	0.83	2.75	0.560	173.06	120.18	12.26	7.33
540A	42°27.69‘ N	03°25.64‘ E	911	0.43	2.25		203.97	160.16	10.22	7.27
540B	42°25.70‘ N	03°41.34‘ E	812	1.22	7	0.750	193.99	151.44	10.24	7.22
540C	41°21.04‘ N	03°01.36‘ E	721	0.97	4.25	0.650	179.74	138.14	9.91	6.84
585	36°39.60‘ N	25°55.72‘ E	708	2.25	21	0.430	151.13	105.86	7.85	4.75
586	36°34.32‘ N	25°57.91‘ E	424	1.00	18	0.408	151.13	105.86	10.83	6.56
589	36°45.19’ N	26°35.38‘ E	584	2.13	14.5	0.698	150.87	105.59	8.84	5.34
592	37°47.65‘ N	26°15.72‘ E	1148	0.38	16	0.630	151.46	110.29	5.81	3.72
595	38°15.63‘ N	25°06.17‘ E	662	0.56	19		159.63	114.32	8.84	5.52
596	38°57.32‘ N	24°45.20‘ E	884	0.41	30	0.730	160.50	116.00	7.43	4.70
599	39°45.36‘ N	24°05.61‘ E	1084	0.47	16.5	0.579	195.88	138.51	8.66	5.31
601	40°05.22‘ N	24°36.62‘ E	977	0.27	6	0.750	206.68	145.42	9.97	6.07
602	40°13.03‘ N	24°15.39‘ E	1466	0.78	4	0.820	236.78	164.09	9.36	5.58
338	36°15.03‘ N	03°24.98‘ W	732	0.55	1.75	0.832	294.00	207.05	19.64	11.98
339	36°18.30‘ N	03°08.39’ W	849	0.81	2.25	0.766	280.09	197.86	16.71	10.24
347	36°27.90‘ N	02°55.50‘ W	629	0.63	1.5	0.835	273.71	192.02	19.53	11.85
394	38°53.39‘ N	02°38.40‘ E	646	1.28	8		171.05	124.55	9.90	6.33
395	38°57.70‘ N	02°31.51‘ E	834	0.81	7	0.463	170.54	125.07	8.40	5.42
396	39°09.60‘ N	02°28.78‘ E	562	0.88	10	0.403	167.82	123.45	10.52	6.82
Canyon ø	42°27.60‘ N	03°29.80‘ E	920	1.50	4	0.870			19.7	19.7
Canyon feb	42°27.60‘ N	03°29.80‘ E	920	0.49						
Canyon aug	42°27.60‘ N	03°29.80‘ E	920	2.50						
Slope ø	42°25.60‘ N	03°42.00‘ E	800	1.81	11	0.720			12.8	12.8
Slope feb	42°25.60‘ N	03°42.00‘ E	800	3.21						
Slope aug	42°25.60‘ N	03°42.00‘ E	800	0.41						

922

923 Table 2.

Site	$\delta^{13}C_{Pari}$ (‰ VPDB)	st. dev. (‰)	$\delta^{13}C_{Cpac}$ (‰ VPDB)	st. dev. (‰)	$\delta^{13}C_{Clob}$ (‰ VPDB)	st. dev. (‰)	$\delta^{13}C_{epi}$ (‰ VPDB)	st. dev. (‰)
537			1.11	0.32			1.11	0.32
540A	1.08	0.14	0.76	0.17			1.08	0.14
540B	0.99		1.01	0.13			1.01	0.11
540C	0.76		1.01	0.09			1.01	0.09
585	1.32	0.24					1.32	0.24
586	1.90	0.15					1.90	0.15
589	1.34	0.11					1.34	0.11
592	1.30	0.23					1.30	0.23
595	1.87	0.15					1.87	0.15
596	0.96	0.04					0.96	0.04
599	1.76	0.12					1.76	0.12
601			0.47	0.06			1.02	0.06
602	0.87		0.31	0.20			0.87	
338	1.22		0.64	0.21	0.92		1.22	
339	1.22	0.11	0.86		-0.12		1.22	0.11
347	1.16	0.07	0.82	0.06	-0.16		1.16	0.07
394			1.52	0.01	0.98		1.28	
395			1.54		0.80	0.02	1.1	0.02
396	1.22	0.22	1.76		0.92		1.22	0.22
Canyon ø			0.52	0.04			0.80	0.07
Slope ø			0.39	0.09			1.00	0.06

924

925 Table 2 (continued)

Site	$\delta^{13}C_{Umed}$ stained (‰ VPDB)	st. dev. (‰)	$\delta^{13}C_{Umed}$ unstained (‰ VPDB)	st. dev. (‰)	$\delta^{13}C_{Umed}$ stained (>600µm) (‰ VPDB)	st. dev. (‰)	$\delta^{13}C_{Umed}$ unstained (>600µm) (‰ VPDB)	st. dev. (‰)	$\Delta\delta^{13}C_{Umed\text{-}Epi}$ stained (>600µm) (‰)	st. dev. (‰)	$\Delta\delta^{13}C_{Umed\text{-}Epi}$ unstained (>600µm) (‰)	st. dev. (‰)
537	0.17	0.38	-0.88	0.16	0.35	0.26	-0.82	0.03	-0.76	0.58	-1.93	0.35
540A	-0.46	0.21			-0.21	0.09			-1.29	0.30		
540B	0.13	0.32	0.19	0.35	0.27	0.23	0.46	0.10	-0.74	0.34	-0.55	0.21
540C	-0.14	0.30	0.06	0.32	0.05	0.26	0.28	0.32	-0.97	0.41	-0.74	0.47
585	0.58	0.22	0.50	0.47	0.58	0.22	0.50	0.22	-0.74	0.46	-0.82	0.46
586			0.95	0.46			1.11	0.31			-0.79	0.46
589			0.51	0.46			0.73	0.39			-0.61	0.50
592	-0.14	0.02	0.15	0.25	-0.12	0.00	0.24	0.20	-1.42	0.23	-1.06	0.43
595	0.09	0.53	0.67	0.41	0.37	0.31	0.77	0.41	-1.49	0.46	-1.09	0.56
596	-0.38	0.38	-0.43	0.34	-0.23	0.33	-0.27	0.27	-1.19	0.37	-1.23	0.31
599	0.03	0.26	0.25	0.45	0.12	0.20	0.41	0.28	-1.63	0.32	-1.35	0.40
601	-0.53	0.27	-0.47	0.38	-0.34	0.14	-0.37	0.35	-1.36	0.20	-1.39	0.41
602	-1.11	0.31	-1.09	0.27	-0.98	0.32	-1.13	0.26	-1.85	0.32	-2.00	0.26
338	-0.05	0.26	0.29	0.37	0.07	0.28	0.55	0.23	-1.15	0.28	-0.67	0.23
339	0.02	0.46	0.06	0.20	0.22	0.28	0.16	0.19	-0.99	0.39	-1.06	0.30
347	-0.19	0.25	0.02	0.17	-0.13	0.13	0.41	0.00	-1.29	0.20	-0.75	0.07
394	0.58	0.31	0.61	0.23	0.64	0.26	0.71	0.13	-0.64	0.27	-0.58	0.14
395	0.47	0.30	0.53	0.21	0.53	0.27	0.63	0.13	-0.57	0.27	-0.46	0.13
396	0.66	0.22	-0.64	0.60	0.72	0.19	-0.91	0.42	-0.50	0.29	-2.13	0.52
Canyon ø	-0.32	0.29	-0.32	0.27	-0.17	0.20	-0.21	0.26	-0.97	0.27	-1.01	0.33
Slope ø	0.26	0.30			0.33	0.26			-0.67	0.32		

926

927 Table 3.

U. mediterranea stained

site	n	linear fit	R-squared	p-value
537	24	Y = 0.001379 * X - 1.810017	0.67	$1.1065*e^{-6}$
540A	23	Y = 0.001007 * X - 1.770373	0.70	$5.746*e^{-7}$
540B	14	Y = 0.001257 * X - 1.7208851	0.54	0.0027
540C	46	Y = 0.000943 * X - 1.639236	0.55	$3.769*e^{-6}$
585	3	Y = -0.00224 * X + 1.222667	1.00	0.0082
592	2	Y = 0.00034 * X - 1.6535	1.00	X
595	10	Y = 0.002013 * X - 3.012139	0.75	0.0012
596	7	Y = 0.001822 * X - 2.490764	0.60	0.0401
599	10	Y = 0.001600 * X - 2.789560	0.49	0.0289
601	11	Y = 0.001322 * X - 2.497314	0.70	0.0013
602	15	Y = 0.001143 * X - 2.709099	0.41	0.0102
338	10	Y = 0.001498 * X - 2.265059	0.72	0.0020
339	12	Y = 0.001527 * X - 2.323114	0.48	0.0124
347	7	Y = 0.001126 * X - 2.119201	0.68	0.0232
394	19	Y = 0.000968 * X - 1.680654	0.27	0.0221
395	23	Y = 0.001509 * X - 2.135640	0.40	0.0012
396	20	Y = 0.000789 * X - 1.304866	0.39	0.0034
Canyon aug	7	Y = 0.000516 * X - 1.297794	0.45	0.1015
Canyon feb	21	Y = 0.000701 * X - 1.634263	0.43	0.0012
Slope aug	6	Y = 0.000671 * X - 1.207976	0.34	0.2244
Slope feb	14	Y = 0.001223 * X - 1.518849	0.48	0.0060

U. mediterranea unstained

site	n	linear fit	R-squared	p-value
537	7	Y = 0.000408 * X - 2.169793	0.33	0.1784
540B	16	Y = 0.001017 * X - 1.457536	0.80	$2.4803*e^{-6}$
540C	9	Y = 0.000938 * X - 1.343878	0.53	0.0270
585	4	Y = 0.001610 * X - 1.910093	0.85	0.0808
586	29	Y = 0.001555 * X - 2.035859	0.48	$2.9156*e^{-5}$
589	25	Y = 0.001612 * X - 1.917381	0.58	$1.0482*e^{-5}$
592	28	Y = 0.001001 * X - 1.826222	0.48	$4.5201*e^{-5}$
595	36	Y = 0.000841 * X - 1.740275	0.17	0.0130
596	37	Y = 0.001065 * X - 2.004262	0.30	0.0005
599	12	Y = 0.001031 * X - 2.201211	0.31	0.0600
601	21	Y = 0.000312 * X - 1.871316	0.04	0.3927
602	14	Y = -0.000427 * X - 1.697763	0.12	0.2159
338	10	Y = 0.001343 * X - 1.735480	0.90	$3.0586*e^{-5}$
339	9	Y = 0.000456 * X - 1.408000	0.31	0.1197
347	10	Y = 0.000615 * X - 1.400530	0.71	0.0023
394	22	Y = 0.000573 * X - 1.221329	0.32	0.0060
395	15	Y = 0.000544 * X - 1.301955	0.33	0.0256
396	17	Y = -0.001682 * X - 1.020989	0.50	0.0016
Canyon aug	36	Y = 0.000584 * X - 1.469912	0.28	0.0009

Figure captions

Figure 1. Location of the study areas in the Mediterranean Sea and regional bathymetric maps with locations of sample sites in the (a) Mallorca Channel, (b) Alboran Sea, (c) Gulf of Lions and Spanish Slope off Barcelona, (d) Strait of Sicily, and (e) Aegean Sea.

Figure 2. (a) The $\delta^{13}C$ of epifaunal species (*Cibicidoides pachydermus*, *Cibicides lobatulus*, *Planulina ariminensis*) for each investigated site. Each symbol represents a single measurement. Red symbols mark relocated or fossil tests that haven't been used to calculate $\delta^{13}C_{Epi}$. Green circles show $\delta^{13}C_{Epi}$ values used as approximation of the $\delta^{13}C$ of bottom water DIC. Details on the selection of tests and procedure for the estimation of $\delta^{13}C_{Epi}$ values are discussed in chapter 4.1. (b) The $\delta^{13}C_{Epi}$ versus water depth shows a wider scattering for the Aegean Sea, than for the Western Mediterranean Sea. Colored lines in the background indicate water mass end members of the Mediterranean Sea after Pierre (1999).

Figure 3. Correlation between $\delta^{13}C_{Umed}$ and $\delta^{13}C_{Epi}$ difference ($\Delta\delta^{13}C_{Umed\text{-}Epi}$) and size classes of *U. mediterranea*. For a better clarity and due to the large number of measured data (see Supplementary Table 1), the linear regressions for each site are given, showing clear ontogenetic trends in $\delta^{13}C_{Umed}$ due to size-independent $\delta^{13}C_{Epi}$ values. The shown data are from live (rose Bengal stained) and dead (unstained) individuals of *U. mediterranea* as well as for the western Mediterranean Sea (left) and Aegean Sea (right). Dashed lines represent already published data (Schmiedl et al., 2004; Theodor et al., 2016).

Figure 4. The $\delta^{13}C$ difference between live *Uvigerina mediterranea* and epifaunal taxa ($\Delta\delta^{13}C_{Umed\text{-}Epi}$) plotted against (a) Median Living Depth (MLD) of *U. mediterranea*, (b) depth of redox boundary in the sediment, (c) total organic carbon (TOC) content of the sediment. The MLD error bars for the canyon and slope sites in the Gulf of Lions reflect the seasonal MLD contrasts of *U. mediterranea* between February and August 1997 (Schmiedl et al., 2004).

Figure 5. The $\delta^{13}C$ difference between live and dead *Uvigerina mediterranea* and epifaunal taxa ($\Delta\delta^{13}C_{Umed\text{-}Epi}$) against organic carbon flux rates (C_{org} flux) calculated from primary productivity in surface waters after Betzer et al. (1984). As in figure 4, satellite derived Primary Production values of Antoine & Morel (1996) (top) and Uitz et al., (2008) (bottom) were used.

Figure 6: Correlation of the $\delta^{13}C$ difference between live *Uvigerina mediterranea* and epifaunal taxa ($\Delta\delta^{13}C_{Umed\text{-}Epi}$) and organic carbon flux rate (C_{org} flux) calculated according to Antoine & Morel (1996) and Betzer et al. (1984). Transparent data from the central and northern Aegean Sea and the Gulf of Lions have been removed from the function since PP-based C_{org} flux values are likely underestimated because of the additional influence of lateral organic matter fluxes on the $\delta^{13}C_{Umed}$ values in these areas.

968 Figure 1

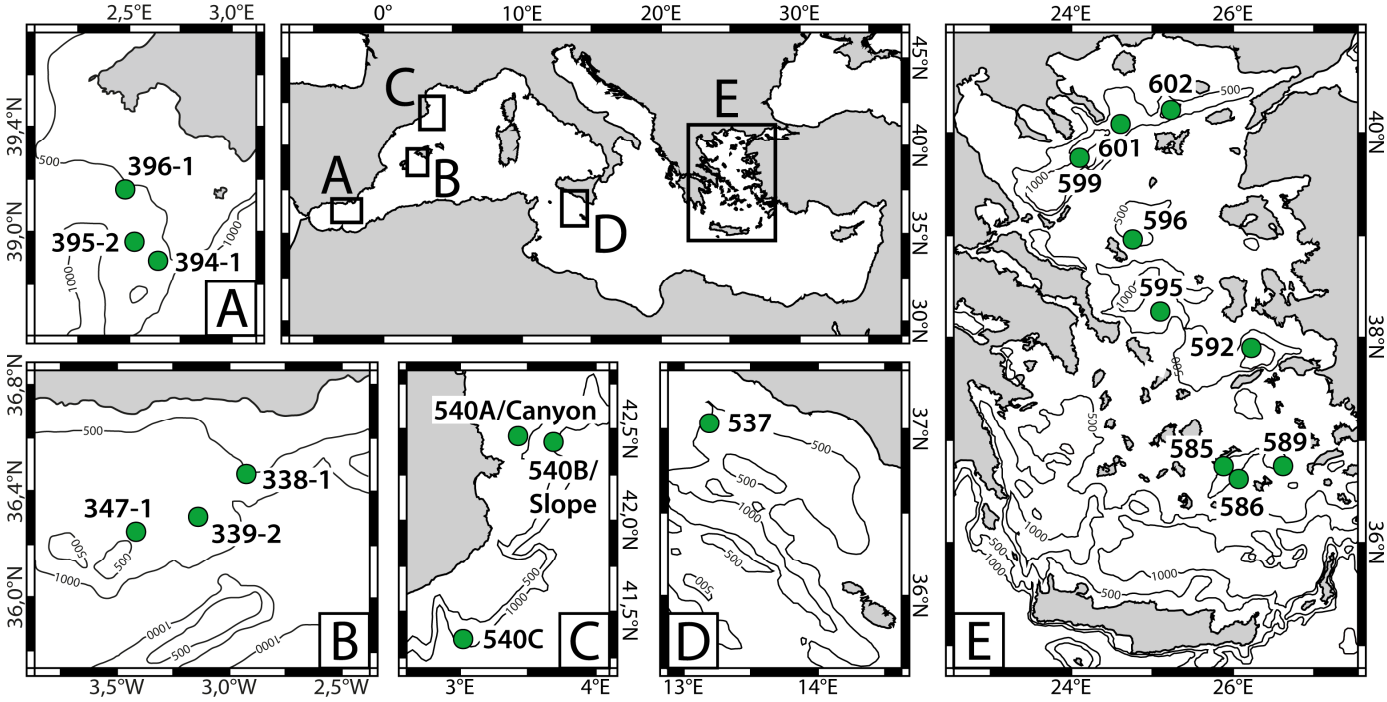

969

970 Figure 2.

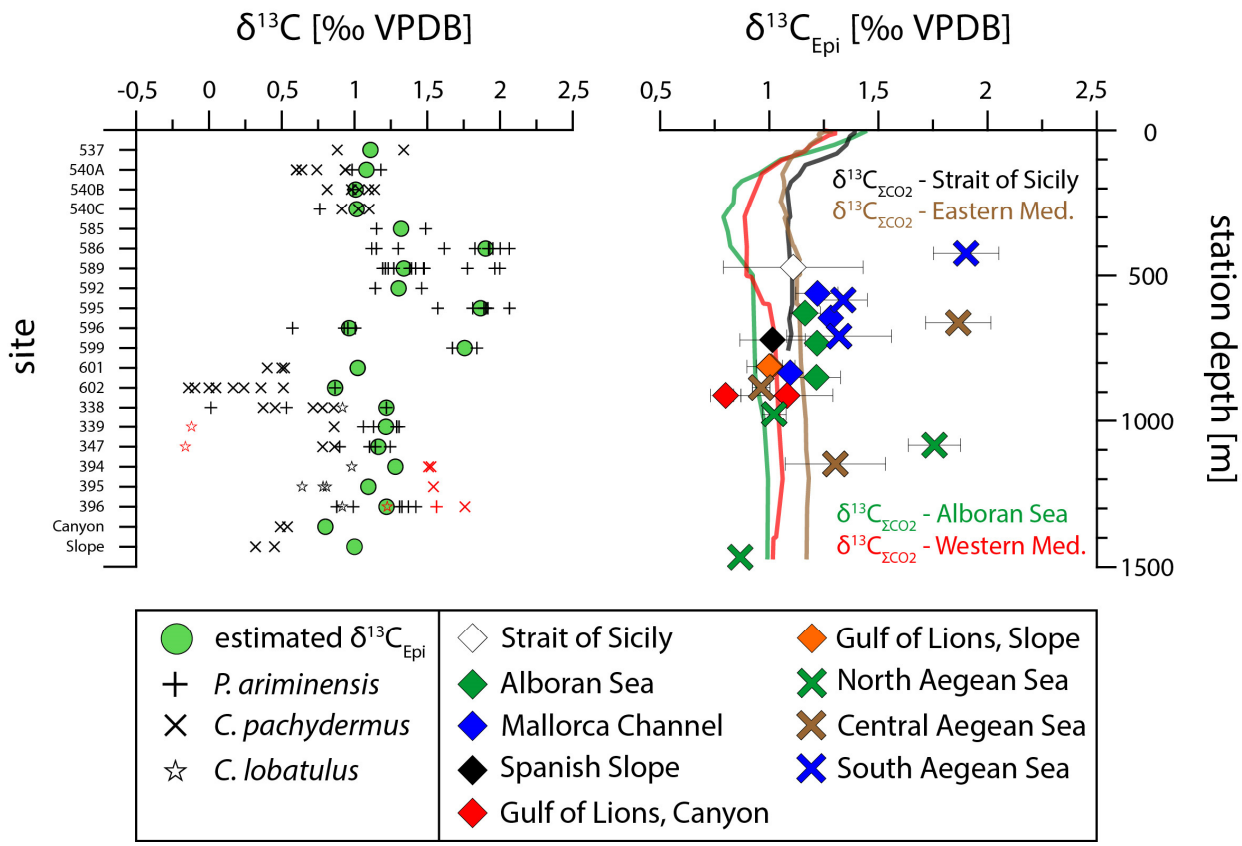

971

972

973 Figure 3.

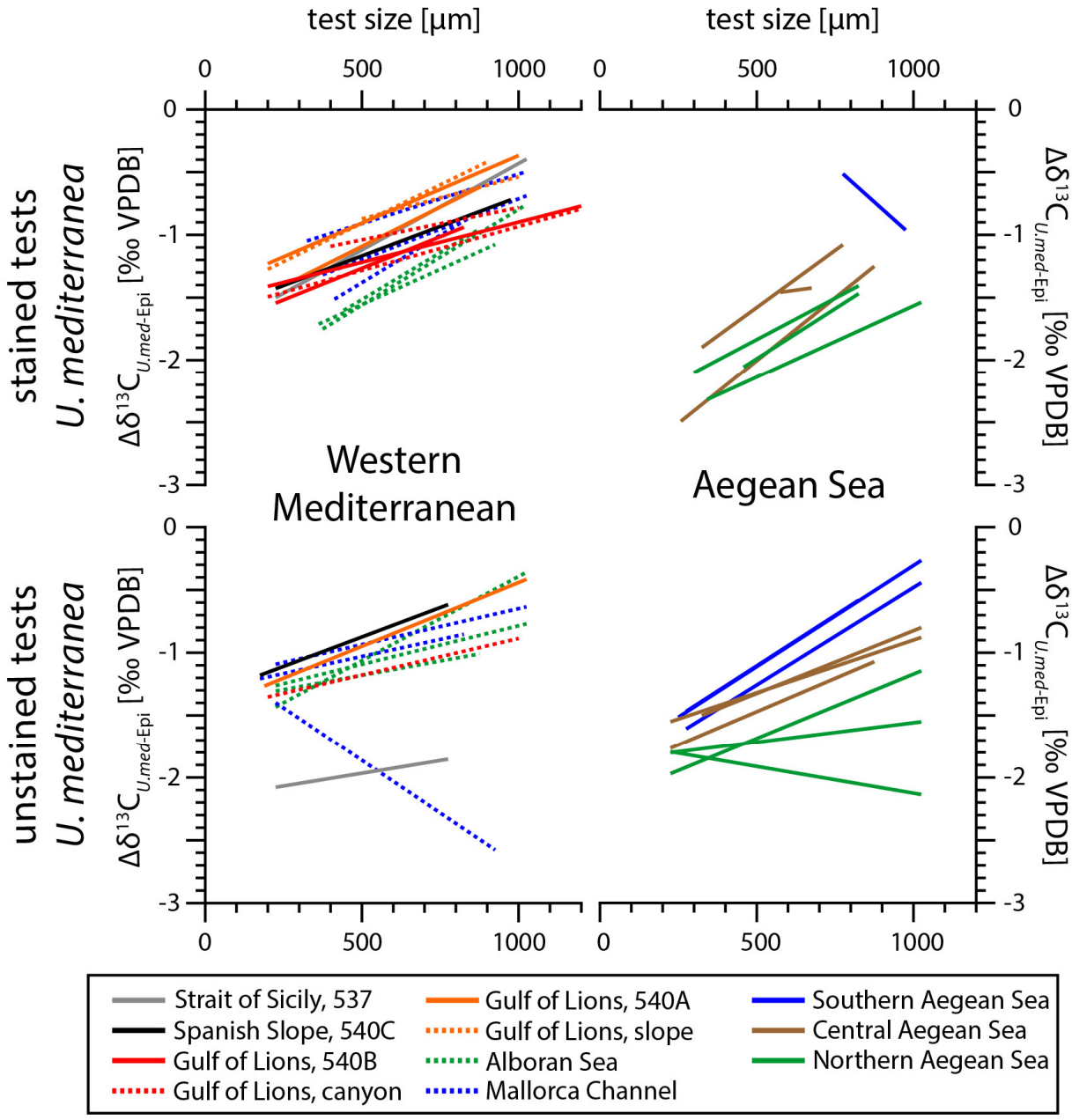

974

975

976 Figure 4.

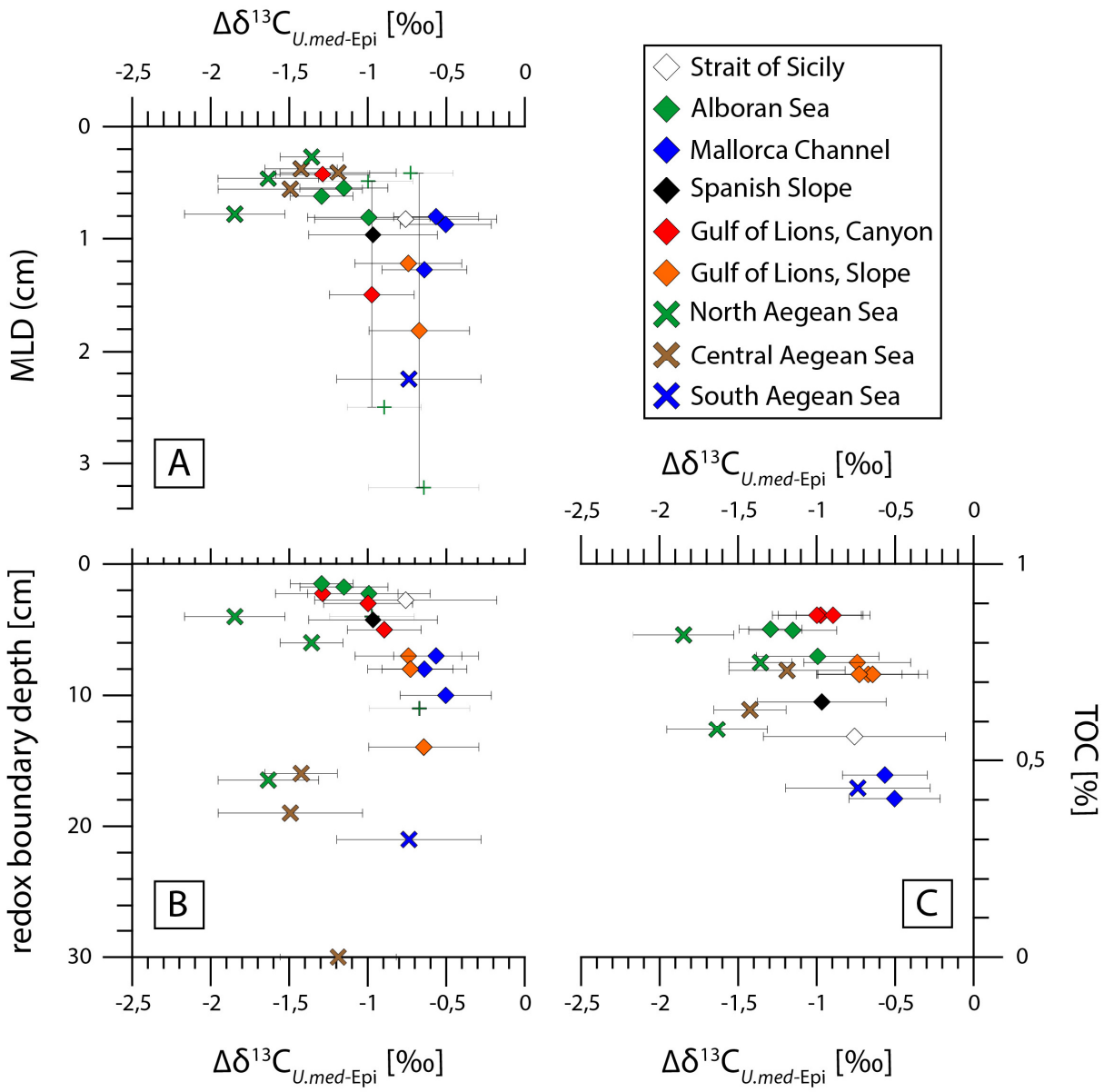

977

978

979 Figure 5.

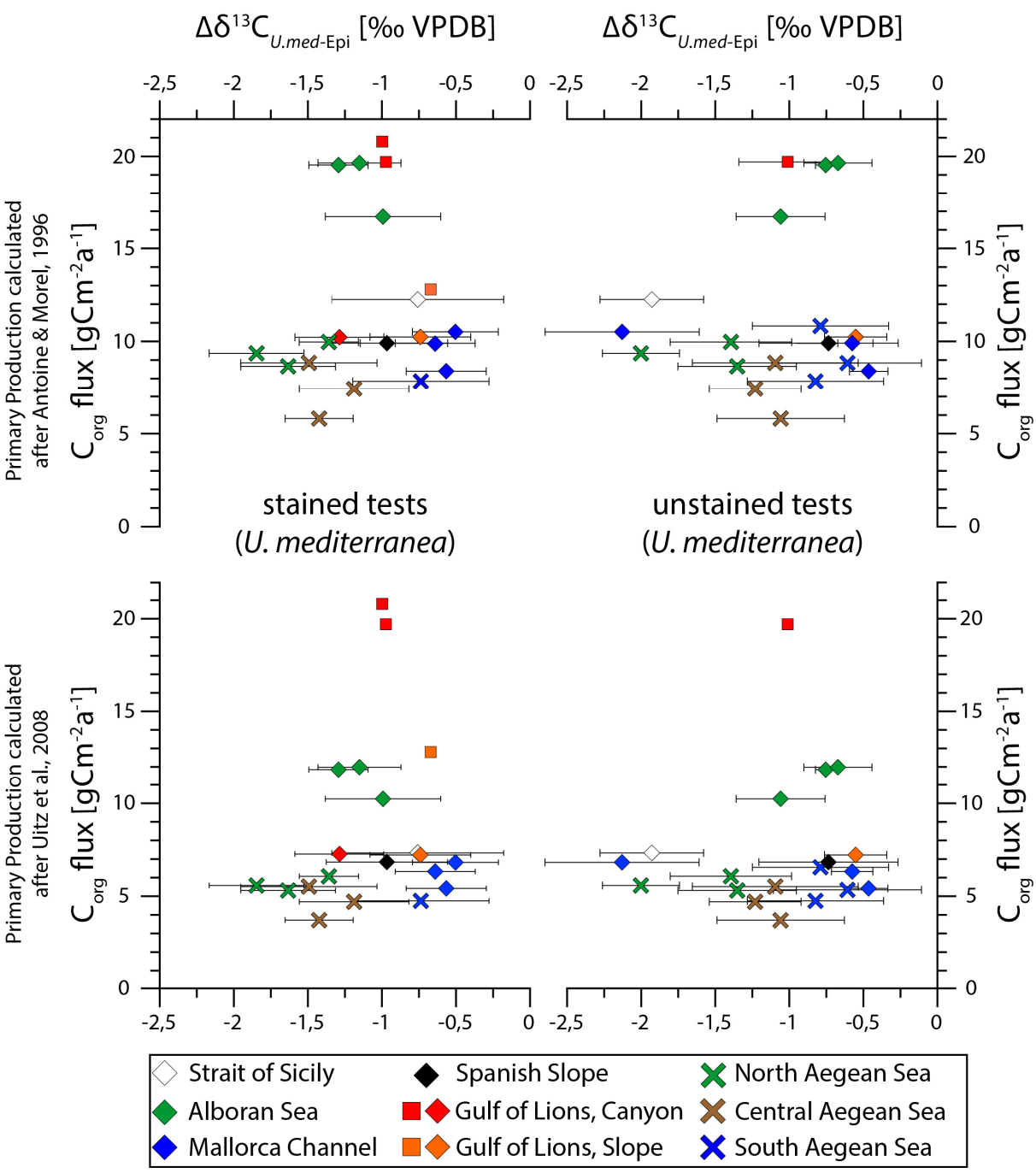

980

981

982 Figure 6.

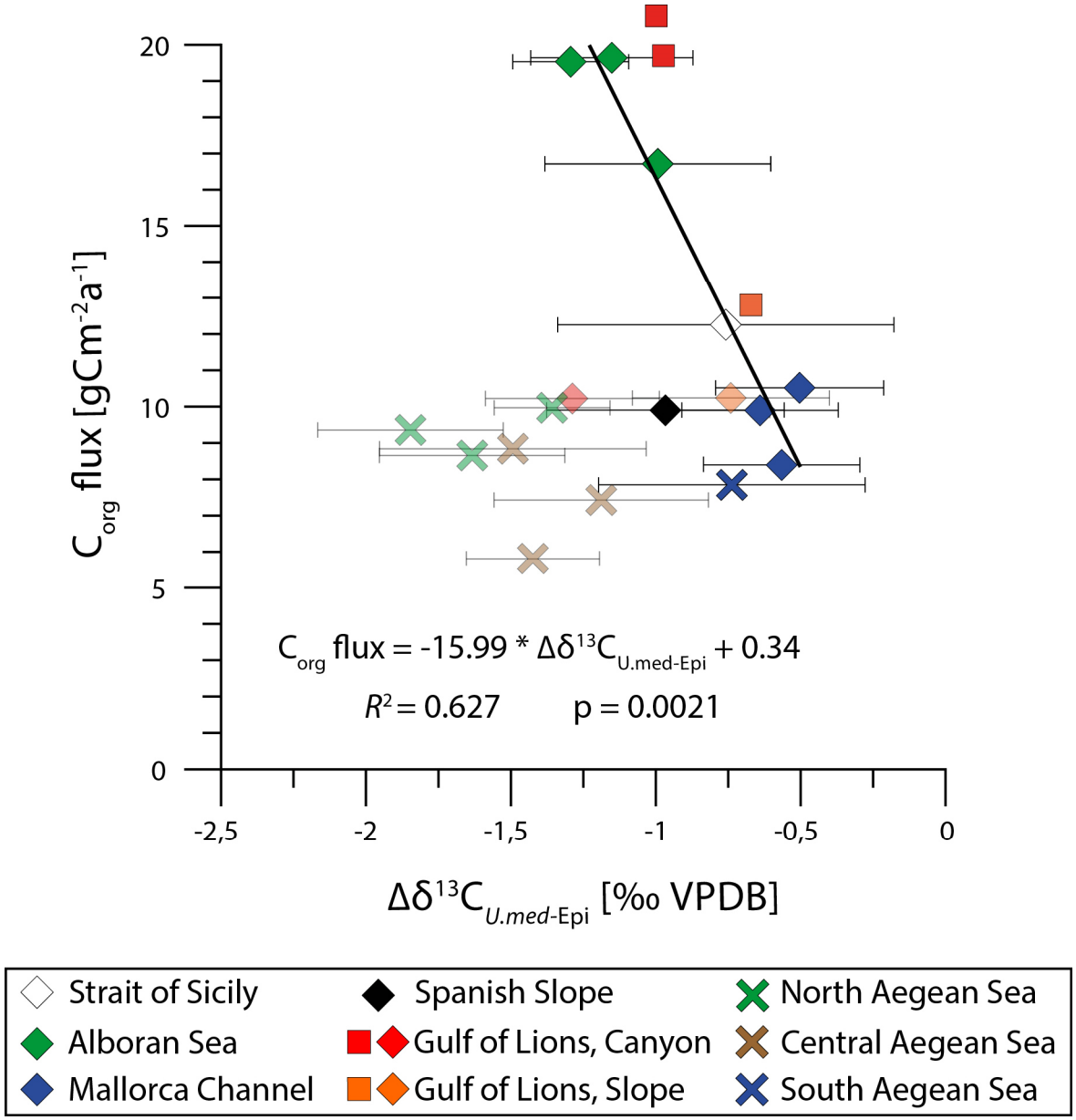

983